A heat-shock response regulated by the PfAP2-HS transcription factor protects human malaria parasites from febrile temperatures

Elisabet Tintó-Font[1], Lucas Michel-Todó[1,#], Timothy J. Russell[2,#], Núria Casas-Vila[1], David J. Conway[3], Zbynek Bozdech[4], Manuel Llinás[2,5] & Alfred Cortés[1,6,*]

[1] ISGlobal, Hospital Clínic - Universitat de Barcelona, Barcelona 08036, Catalonia, Spain

[2] Department of Biochemistry & Molecular Biology and Huck Center for Malaria Research, Pennsylvania State University, University Park 16802, PA, USA

[3] Department of Infection Biology, London School of Hygiene and Tropical Medicine, London, WC1E 7HT, UK

[4] School of Biological Sciences, Nanyang Technological University, Singapore 637551, Singapore

[5] Department of Chemistry, Pennsylvania State University, University Park 16802, PA, USA

[6] ICREA, Barcelona 08010, Catalonia, Spain

[#] Equal contribution as second author

* Correspondence: alfred.cortes@isglobal.org (Alfred Cortés)

Periodic fever is a characteristic clinical feature of human malaria, but how parasites survive febrile episodes is not known. Although *Plasmodium* spp. genomes encode a full set of chaperones, they lack the conserved eukaryotic transcription factor HSF1, which activates the expression of chaperones upon heat-shock. Here, we show that PfAP2-HS, a transcription factor in the ApiAP2 family, regulates the protective heat-shock response in *Plasmodium falciparum*. PfAP2-HS activates transcription of *hsp70-1* and *hsp90* at elevated temperatures. The main binding site of PfAP2-HS in the entire genome coincides with a tandem G-box DNA motif in the *hsp70-1* promoter. Engineered parasites lacking PfAP2-HS have reduced heat-shock survival and severe growth defects at 37ºC, but not at 35ºC. Parasites lacking PfAP2-HS also have increased sensitivity to imbalances in protein homeostasis (proteostasis) produced by artemisinin, the frontline antimalarial drug, or by the proteasome inhibitor epoxomicin. We propose that PfAP2-HS contributes to maintenance of proteostasis under basal conditions and upregulates specific chaperone-encoding genes at febrile temperatures to protect the parasite against protein damage.

INTRODUCTION

A temperature increase of only a few degrees Celsius above the optimal growth temperature of any organism causes aberrant protein folding and aggregation, which contributes to an imbalance in proteostasis that can lead to cell-cycle arrest or cell death[1]. To counteract the effect of high temperatures and other

proteotoxic conditions, cells have a well-characterized heat-shock response that induces expression of molecular chaperones that aid protein refolding and prevent non-specific protein aggregation[1,2]. In most eukaryotes, the immediate upregulation of chaperone-encoding genes during heat-shock depends on the conserved transcription factor HSF1, whereas other transcriptional changes during thermal stress are driven by different transcription factors[3-6].

The human response to blood-stage infection with malaria parasites involves periodic fever episodes, which are the hallmark of clinical malaria[7-9]. Fever is an important part of the human innate immune response, and it may contribute to reducing the total parasite burden[8-10]. Infection with *P. falciparum*, which causes the most severe forms of human malaria, results in fevers that typically occur on alternate days (tertian fever). Tertian fever reflects the ~48 h duration of the asexual intraerythrocytic development cycle (IDC), during which parasites progress through the ring, trophozoite and multinucleated schizont stages. Fever episodes are triggered by schizont rupture and release of invasive merozoites[8,9]. In vitro, febrile temperatures inhibit parasite growth, with maximal effect on trophozoites and schizonts[9,11,12], and also induce conversion of asexual parasites into sexual forms that mediate transmission to mosquitoes[13].

Despite the importance of the heat-shock response for human malaria parasite survival during host fever episodes, the regulation of the heat-shock response has not been characterized in these organisms. The genomes of *Plasmodium* spp. lack an ortholog of HSF1, but they encode the main chaperone families described in other organisms[14], and several specific *P. falciparum* chaperones have been shown to be essential for heat-shock survival

[15-19]. Phosphatidylinositol 3-phosphate and apicoplast-targeted pathways are also essential for parasite survival under thermal stress[18,19]. Transcript levels of over three hundred genes are altered at febrile temperatures[20], but how these transcriptional changes are regulated is not known. Here we set out to characterise the regulation of the protective response of *P. falciparum* to increased temperature.

RESULTS

A nonsense mutation in *pfap2-hs* is associated with low survival from heat-shock

To understand the molecular basis of heat-shock resistance in *P. falciparum*, we first analysed parasite lines that had been previously selected with periodic heat-shock for five consecutive rounds of the IDC[21] (Fig. 1a). Although the parental parasite line (3D7-A) appeared to have lost the ability to withstand heat-shock (~30% survival to a 3 h heat-shock at 41.5ºC) during growth in vitro, it re-adapted to heat-shock pressure (>75% heat-shock survival) in only three generations[21], suggesting that this line contained a selectable subpopulation of parasites resistant to heat-shock. In order to evaluate whether the heat-shock resistance phenotype of 3D7-A had a genetic or an epigenetic basis, we first analysed the transcriptome across the full IDC under basal conditions (no heat-shock) of two independently selected lines (3D7-A-HS r1 and r2) and non-selected cultures maintained in parallel (3D7-A r1 and r2). This analysis failed to identify any basal transcript level differences that could explain the heat-shock resistance phenotypes (Extended Data Fig. 1). Therefore, we sequenced the

genomes of these lines, which revealed a novel single nucleotide polymorphism (SNP) that was predominant in non-selected cultures, but virtually absent after heat-shock selection (Fig. 1b-c, Supplementary Table 1). The mutation is also absent from two other 3D7 stocks in our laboratory and from the 3D7 reference genome, indicating that it arose spontaneously in the 3D7-A stock during culture. This SNP results in a premature STOP codon (Q3417X) in the gene PF3D7_1342900, which encodes a putative transcription factor of the ApiAP2 family[22-24] that we termed PfAP2-HS. PfAP2-HS has three AP2 domains (D1-D3), and the Q3417X mutation results in a truncated protein that lacks D3 (PfAP2-HSΔD3) (Fig. 1d). This result indicates that adaptation of 3D7-A to heat-shock involved selection of parasites expressing full-length PfAP2-HS, consistent with a role for this protein in the heat-shock response. In support of this idea, the first AP2 domain (D1) of PfAP2-HS was previously reported to recognize in vitro a DNA motif termed G-box[23], which is enriched in the upstream region of some heat-shock protein (HSP) chaperone genes[25].

To test the involvement of PfAP2-HS in heat-shock resistance, we used a heat-shock survival assay with a 3 h heat-shock at 41.5ºC[21] at the mature trophozoite stage, because maximal survival differences between heat-shock sensitive and resistant parasite lines were observed when exposing parasites at this stage (Fig. 1e). The analysis of a collection of 3D7-A subclones revealed that all subclones with the Q3417X mutation (e.g., 10G subclone) have a heat-shock-sensitive phenotype, whereas subclones with the wild-type allele (e.g., 10E subclone) have a heat-shock resistant phenotype (Fig. 1a,f).

Deletion of PfAP2-HS reduces survival from heat-shock

To further characterize PfAP2-HS, we sought to disrupt the entire gene using CRISPR-Cas9 technology. After several unsuccessful attempts with different 3D7 subclones at 37ºC (the physiological temperature for *P. falciparum*), we reasoned that PfAP2-HS may play a role in regulating the expression of chaperones under basal conditions, in addition to being necessary for heat-shock survival. Therefore, we attempted to knock out the gene in cultures maintained at 35ºC, as mild hypothermia is expected to reduce protein unfolding and favour proteome integrity[26,27]. Indeed, at 35ºC, knockout of *pfap2-hs* was readily achieved in both the heat-shock-resistant 10E and the heat-shock-sensitive 10G subclones of 3D7-A (10E_Δ*pfap2-hs* and 10G_Δ*pfap2-hs* lines) (Fig. 1a,d, Extended Data Fig. 2a). Deletion of *pfap2-hs* resulted in severely increased sensitivity to heat-shock, with a level of heat-shock survival below that of parasites expressing PfAP2-HSΔD3. Deletion of the gene in two additional parasite lines of unrelated genetic background, HB3 and D10, also resulted in a major reduction in heat-shock survival (Fig. 1g).

The PfAP2-HS-driven transcriptional response to heat-shock is extremely compact

To define the PfAP2-HS-dependent and independent heat-shock response, we carried out a time-course transcriptome analysis of the 10E (wild-type PfAP2-HS), 10G (PfAP2-HSΔD3) and 10E_Δ*pfap2-hs* lines during and after heat-shock (Fig. 2a, Extended Data Fig. 3a, Supplementary Table 2). Hierarchical clustering based on changes in cultures exposed to heat-shock compared with control cultures maintained in parallel without heat-shock revealed one cluster

of transcripts (cluster I) that are rapidly increased during heat-shock in 10E but not in 10G or 10E_Δ*pfap2-hs*. Cluster I comprises only three genes: a gene of unknown function (PF3D7_1421800), the cytoplasmic *hsp70* (*hsp70-1*; PF3D7_0818900) and *hsp90* (PF3D7_0708400) (Fig. 2a). The regulatory regions of these two chaperone-encoding genes contain the best two matches in the full genome for a tandem G-box[23,25] (Extended Data Fig. 3b). While hundreds of genes in the *P. falciparum* genome contain a single G-box, only *hsp70-1* and *hsp90* showed PfAP2-HS-dependent activation during heat-shock, suggesting that the tandem G-box arrangement may be needed for activation by PfAP2-HS. The strongest transcriptional response to heat-shock was observed for *hsp70-1* (~16-fold increase versus ~4-fold for *hsp90*).

To validate the observation that rapid activation of the cluster I genes upon heat-shock depends on PfAP2-HS and requires its D3, we analysed the heat-shock response of *pfap2-hs* knockout parasite lines of different genetic backgrounds and several 3D7-A mutant subclones expressing PfAP2-HSΔD3 (Extended Data Fig. 4). In all knockout and mutant lines examined, the *hsp70-1* response to heat-shock was delayed and of reduced magnitude. These experiments also confirmed that the *hsp90* response is weaker than the *hsp70-1* response, and is delayed in PfAP2-HS mutants.

PfAP2-HS-independent transcriptome alterations induced by heat-shock

Genes in other clusters (II-VI) of our transcriptomic analyses showed changes in expression during heat-shock that were independent of PfAP2-HS; these changes were more pronounced in the mutant than in the wild type lines (Fig. 2a). Indeed, more genes with altered transcript levels were identified in the

heat-shock sensitive 10G and 10E_Δ*pfap2-hs* lines than in 10E (Fig. 2b). Furthermore, the alterations in clusters II-VI transcripts persisted 2 h after heat-shock in both heat-shock-sensitive lines, whereas in 10E the majority of transcripts returned to basal levels (Fig. 2a). This suggests that many of these altered transcripts reflect unresolved cell damage or death. In 10E, the rapid PfAP2-HS-dependent response may protect cells from damage and enable rapid recovery from heat shock, thus limiting (in magnitude and duration) the changes in the expression of clusters II-VI genes that reflect cell damage. Indeed, after heat-shock the transcriptome of the 10G and 10E_Δ*pfap2-hs* lines showed a more pronounced deviation from a reference transcriptome[28] than 10E (Fig. 2c). Global transcriptional analysis also revealed that heat-shock resulted in delayed IDC progression, again more pronounced in 10G and 10E_Δ*pfap2-hs* than in 10E (Fig. 2d).

In addition to genes reflecting cell damage, clusters II-VI likely include some genes that participate in the PfAP2-HS-independent heat-shock response. In particular, clusters V-VI include several chaperone-encoding genes upregulated during heat-shock, although at a later time point than cluster I genes (Fig. 2a). However, the expression of the majority of known *P. falciparum* chaperones[14] was not altered by heat-shock and, except for cluster I genes, the alterations occurred mainly in the mutant lines (Extended Data Fig. 5). To provide a clearer view of the wild-type heat-shock response, we analysed changes upon heat-shock in the 10E line alone. Overall, there was generally good concordance with the genes and processes altered upon heat-shock described in a previous study using non-synchronized cultures[20] (Extended Data Fig. 6, Supplementary Table 3). Altogether, we conclude that a number of

genes are up or downregulated during heat-shock and some may contribute to heat-shock protection through PfAP2-HS-independent responses, but in the absence of the rapid PfAP2-HS-dependent activation of cluster I genes these responses are insufficient to ensure parasite survival at febrile temperatures.

Genome-wide analysis of PfAP2-HS binding sites

To determine the genome-wide occupancy of PfAP2-HS, we analysed a parasite line expressing endogenous HA-tagged PfAP2-HS (Extended Data Fig. 2b) using chromatin immunoprecipitation followed by sequencing (ChIP-seq). The main binding site of PfAP2-HS coincides with the position of the tandem G-box in the upstream region of *hsp70-1* (Fig. 2e, Extended Data Fig. 7, Supplementary Table 4). This is the only binding site with a median fold-enrichment >10 (ChIP versus input) that was consistently detected in five independent ChIP-seq biological replicates, revealing an extremely restricted distribution of PfAP2-HS binding. Similar enrichment was observed in control and heat-shock conditions using ChIP-seq and ChIP-qPCR (Extended Data Fig. 7), which suggests that PfAP2-HS binds constitutively to this site and is activated *in situ* by heat-shock. This is reminiscent of yeast HSF1, which binds the promoter of *hsp70* and most of its other target promoters under both basal and heat-shock conditions[5]. Enrichment for PfAP2-HS at the *hsp90* promoter also coincided with the position of the G-box but was weaker and a significant peak at this position was called in only one of the replicates (Fig. 2e, Extended Data Fig. 7, Supplementary Table 4). No enrichment was observed at the promoter of cluster I gene PF3D7_1421800, which lacks a G-box motif. The only other site consistently enriched for PfAP2-HS binding, albeit at much lower

levels than *hsp70-1*, was the small nucleolar RNA *snoR04* (PF3D7_0510900) locus (Extended Data Fig. 7), which also lacks a G-box and was not upregulated during heat-shock.

Growth defects under basal conditions in parasite lines mutated for PfAP2-HS

Both knockout lines of 3D7 origin (10E_Δ*pfap2-hs* and 10G_Δ*pfap2-hs*) showed severe temperature-dependent growth defects in the absence of heat-shock. They grew at similar rates to the parental lines at 35ºC, but their growth was markedly reduced at 37ºC or 37.5ºC (Fig. 3a). The D10_Δ*pfap2-hs* line also had clearly reduced growth at 37ºC compared to 35ºC, whereas the HB3_Δ*pfap2-hs* line did not (Fig. 3b). Both 3D7 Δ*pfap2-hs* lines also showed a reduced number of merozoites per schizont, especially at 37ºC or 37.5ºC (Fig. 3c), which partly explains the reduced growth rate. Additionally, even at 35ºC, the duration of the IDC was ~4 h longer in both knockout lines (Fig. 3d), which is reminiscent of the slower life cycle progression observed in parasites under proteotoxic stress[29]. In contrast, no growth rate or life cycle duration differences were observed between the 10G (PfAP2-HSΔD3) and 10E lines, indicating that D3 is necessary for heat-shock survival but not for growth under nonstress (37ºC) conditions (Fig. 3a,c-d). Normal growth at 37ºC but low heat-shock survival was also observed in transgenic lines in which bulky C-terminal tags were added to the C-terminus of endogenous PfAP2-HS, suggesting interference of the tag with the function of D3, located only 18 amino acids from the end of the protein (Fig. 1a, Extended Data Fig. 2).

Genome-wide sequence analysis has previously found that nonsense mutations arise in *pfap2-hs* during adaptation to culture conditions[30,31], but are virtually absent from clinical isolates (in the www.malariagen.net/data/pf3k-5 dataset[32], only one out of >2,500 isolates carries a high-confidence SNP resulting in a premature stop codon). The lack of mutations observed in clinical isolates suggests that there is a selection against loss-of-function mutations in PfAP2-HS during human infections, where parasites are frequently exposed to febrile conditions. We exposed a culture-adapted isolate in which ~50% of the parasites carried a mutation that results in truncation of PfAP2-HS before its first AP2 domain[30] (monoclonal Gambian Line 1, PfAP2-HS_ΔD1-3) to one round of heat-shock (41.5 ºC, 3 h), and found that at the next generation only ~20% of the parasites carried the mutation. In control cultures maintained in parallel without heat-shock, the frequency of the mutation remained stable (Fig. 4a-b). This result indicates strong selection by heat-shock against parasites carrying the PfAP2-HS truncation. In contrast, there was relatively weak selection against mutants during culture either at 35ºC or 37ºC, as the prevalence of the mutation only decreased from ~50% to ~20% after culturing for 23 generations at either temperature (Fig. 4c). Consistent with these results, a subclone carrying the mutation (1H) was more sensitive to heat-shock than a wild-type subclone (4E), but both showed no measurable difference in growth at 35ºC or 37ºC (Fig. 4d-f). Together, these results indicate that PfAP2-HS is essential for heat-shock survival in all the genetic backgrounds tested. However, PfAP2-HS is necessary for normal progression through the IDC at 37ºC in only specific genetic backgrounds (i.e., 3D7 and D10), whereas in others (HB3 and the Gambian isolate) it is not essential.

Transcriptional alterations in parasites lacking PfAP2-HS under basal conditions

To gain insight on the molecular basis of the growth defects of some of the knockout lines, we compared the trophozoite transcriptome of 10E_Δ*pfap2-hs* with that of the parental 10E under basal (no heat-shock) conditions. This revealed only a small set of genes with a ≥2 fold-decrease in transcript levels, which included *hsp70-1*, the direct PfAP2-HS target *snoR04* RNA and several genes mainly involved in ribosome formation. Transcript levels for *hsp90* were also reduced (<2 fold-decrease) in the knockout line (Extended Data Fig. 8a-b, Supplementary Table 2). Reduced *hsp70-1* and *hsp90* transcript levels under basal conditions in 10E_Δ*pfap2-hs* mature trophozoites were independently confirmed by reverse transcription–quantitative PCR (RT-qPCR), and also observed at the late ring stage and in the knockout lines of D10 and HB3 genetic background (Extended Data Fig. 8c). These results indicate that PfAP2-HS contributes to regulating the basal expression of the same chaperone-encoding genes that it activates upon heat-shock, among a few other genes. Together with the observation that the growth defect of the *pfap2-hs* knockout lines is attenuated at 35ºC, this suggests that knockout parasites have reduced proteostasis capacity, such that at 37ºC they are at the edge of proteostasis collapse. Parasite lines that can grow normally at 37ºC in spite of PfAP2-HS deletions including the three AP2 domains therefore must have alternative pathways active to ensure basal proteostasis. We hypothesise that mutant parasites expressing truncated PfAP2-HS are frequently selected under culture conditions because the truncations do not pose a fitness cost at 37ºC in the

lines in which they appear, and they prevent unnecessary activation of the heat-shock response, which can be detrimental[33], by unintended mild stress that may occur during culture.

PfAP2-HS-deficient parasites show increased sensitivity to artemisinin

Artemisinins are potent antimalarial drugs that kill parasites by causing general protein damage[34,35]. Resistance to artemisinin is associated with mutations in the Kelch13 protein[36,37] and involves cellular stress response pathways such as the ubiquitin/proteasome system and the ER-based unfolded protein response (UPR)[34,35,38,39]. Since PfAP2-HS regulates the expression of key chaperones, we tested the sensitivity of PfAP2-HS-deficient lines to dihydroartemisinin (DHA), the active metabolite of artemisinins. In all four different genetic backgrounds (3D7, D10, HB3 and Gambian isolate), knockout of *pfap2-hs* (or truncation before D1) resulted in higher sensitivity to a pulse of DHA than in lines with full PfAP2-HS, both at the ring or the trophozoite stage, whereas 10G showed increased sensitivity only when exposed at the trophozoite stage (Fig. 5a). These results indicate that deletion of PfAP2-HS renders parasites more sensitive to chemical proteotoxic stress, in addition to heat-shock, likely as a consequence of basal defects in cellular proteostasis. We reasoned that if parasites lacking the PfAP2-HS protein bear constitutive proteome defects, they should have low tolerance to disruption of other factors involved in proteostasis maintenance. Indeed, the 10E_Δ*pfap2-hs* line was more sensitive to the proteasome inhibitor epoxomicin than the parental 10E line or the 10G line (Fig. 5b). Furthermore, after heat-shock, there was more accumulation of polyubiquitinated proteins in the knockout line than in 10E or 10G, reflecting

higher levels of unresolved protein damage (Extended Data Fig. 9a). We also assessed the links between the PfAP2-HS-driven heat-shock response and the other main cell stress response pathway, the UPR. Using phosphorylation of eIF2α as a UPR marker, we found that the UPR does not depend on PfAP2-HS and is not directly activated by heat-shock, because the marker was significantly elevated after heat-shock only in the knockout line (Extended Data Fig. 9b).

DISCUSSION

Our results show that the PfAP2-HS transcription factor is bound to the tandem G-box DNA motif in the promoter of the chaperone-encoding gene *hsp70-1* and in response to febrile temperatures rapidly upregulates the expression of this gene and, to a lesser extent, *hsp90* (Fig. 6a). Binding of PfAP2-HS to the G-box is mediated by D1[23], but rapid activation of *hsp70-1* and *hsp90* during heat-shock requires D3, which is not capable of binding DNA in vitro[23] and likely participates in protein-protein interactions or dimerization within the cell[40]. Other components of the protein folding machinery necessary for heat-shock survival[15-17,19] are either constitutively expressed or induced later, but the rapid PfAP2-HS-driven response is essential to avoid irreversible damage. Importantly, parasites lacking either the entire PfAP2-HS or its D3 cannot survive heat-shock.

Although the sequence and domain organization of PfAP2-HS does not show any similarity with HSF1, the conserved master regulator of the heat-shock response in most eukaryotes, from yeast to mammals[3,6], it serves an analogous role. HSF1 regulates a compact transcriptional program that includes

the *hsp70* and *hsp90* genes[4,5]. In yeast, the only essential role of this transcription factor is activating *hsp70* and *hsp90*[5], the same chaperone-encoding genes activated by PfAP2-HS during heat-shock. In addition to its role in the protective heat-shock response, PfAP2-HS is essential for growth at 37ºC in some *P. falciparum* genetic backgrounds. The function of PfAP2-HS under basal conditions is independent of its D3. Several lines of evidence suggest that the role for PfAP2-HS under basal conditions involves proteostasis maintenance (Fig. 6a), similar to yeast HSF1[5]. In other organisms, the heat-shock response mediates protection against different types of proteotoxic stress, in addition to high temperature[1,3]. Here we report that parasites lacking PfAP2-HS have increased sensitivity to artemisinin, and future research will be needed to establish the precise role of the *P. falciparum* heat-shock response in protection against different types of stress. We note that orthologs of *pfap2-hs* are present in all *Plasmodium* spp. analysed (Fig. 6b-c and Extended Data Fig. 10), including murine *Plasmodium* species that do not induce host fever. This observation suggests that, at least in these species, the heat-shock response regulated by AP2-HS may play a role in protection against different conditions.

Finally, while several ApiAP2 transcription factors regulate life cycle transitions in malaria parasites[24,41-43], PfAP2-HS controls a protective response to a within-host environmental challenge. Our findings that the PfAP2-HS transcription factor regulates the activation of a protective heat-shock response settles the long-standing question of whether malaria parasites can respond to changes in within-host environmental conditions with specific transcriptional responses[44].

ONLINE METHODS

Parasite cultures. The 3D7-A stock of the clonal *P. falciparum* line 3D7[45], the 3D7-A subclones 10G, 1.2B, 10E, 4D, 6D, 1.2F, W4-1, W4-2, W4-4 and W4-5[46,47], the HB3B[48] (mosquito and chimpanzee-passaged HB3, provided by Osamu Kaneko, Ehime University, Japan) and D10[49] (provided by Robin F. Anders, La Trobe University, Australia) clonal parasite lines, and the culture-adapted Line 1 from The Gambia[30] have been previously described. The heat-shock-selected lines 3D7-A-HS r1 and r2 were derived from 3D7-A by exposing cultures to a 3 h heat-shock (41.5ºC) at the trophozoite stage for five consecutive cycles (each replicate, r1 and r2, is a fully independent selection from the 3D7-A stock), and the 3D7-A r1 and r2 lines are cultures maintained in parallel at 37ºC without heat-shock[21]. Parasites were cultured in B+ erythrocytes at a 3 % haematocrit under standard culture conditions in RPMI-based media containing Albumax II (without human serum), in a 5% CO_2, 3% O_2, balance N_2 atmosphere (except for cultures for ChIP-seq experiments, in which O+ erythrocytes were used). Regular synchronization was performed using 5 % sorbitol lysis, whereas tight synchronization (1, 2 or 5 h age window) was achieved by Percoll purification followed by sorbitol treatment 1, 2 or 5 h later. All cultures were regularly maintained at 37ºC, with the exception of the *pfap2-hs* knockout lines that were maintained at 35ºC. For experiments performed in parallel with the knockout lines and other parasite lines, all cultures were maintained at 35ºC for at least one cycle before the experiment.

Generation of transgenic parasite lines. We used two single guide RNAs (hereafter referred to as sgRNA or guide) to knockout *pfap2-hs* (11,577 bp)

using the CRISPR/Cas9 system[50] (Extended Data Fig. 2a, Supplementary Table 5). One guide targets a sequence near the 5' end of the gene (position 866-885 from the start codon) whereas the other recognizes a sequence near the 3' end (positions 11,486-11,505). The 5' guide was cloned into a modified pL6-*egfp* donor plasmid[50] in which the *yfcu* cassette had been removed by digestion with *Not*I and *Sac*II, end blunting and re-ligation. 5' and 3' homology regions (HR1: positions -2 to 808 of the gene; HR2: positions +11,520 of the gene to 490 bp after the STOP codon) were also cloned in this plasmid, flanking the *hdhfr* expression cassette, to generate plasmid pL7-pfap2hs_KO_sgRNA5'. The 3' guide was cloned into a modified version of the pDC2-Cas9-U6-hdhfr[51] plasmid, in which we previously removed the *hdhfr* expression cassette by digesting with *Nco*I and *Sac*II, end blunting and re-ligation, and replaced the *Bbs*I guide cloning site by a *BtgZ*I site. The resulting plasmid was named pDC2_wo/hdhfr_pfap2hs_sgRNA3'. All guides were cloned using the In-Fusion system (Takara) as described[50], whereas homology regions were PCR-amplified from genomic DNA and cloned by ligation using restriction sites *Spe*I and *Afl*II (HR1), and *EcoR*I and *Nco*I (HR2).

For constructs aimed at C-terminal tagging of *pfap2-hs* using CRISPR/Cas9 (10E_*pfap2-hs*_eYFP-Cterm and 10E_*pfap2-hs*_3xHA-Cterm lines) we used a guide corresponding to positions 11,508-11,527 of the gene (Extended Data Fig. 2b-c, Supplementary Table 5). The guide was cloned in the pDC2-Cas9-U6-hdhfr[51] plasmid to obtain pDC2_pfap2hs_sgRNA-C. The donor plasmid for tagging with eYFP (pHR-C_pfap2hs_eYFP) was based on plasmid pHRap2g-eYFP[52], with the *pfap2-g* homology regions and *hsp90* 3' sequence replaced by

pfap2-hs homology regions. The 5' homology region (HR1) was generated with a PCR-amplified fragment spanning from nucleotide 10,964 to the sequence of the guide (recodonized), and a 47 bp fragment (generated by annealing two complementary oligonucleotides) consisting of a recodonized version of the remaining nucleotides to the end of the gene. The two fragments were cloned simultaneously, using the In-Fusion system, into *Spe*I-*Bgl*II sites. The 3' homology region (HR2) was a PCR fragment spanning position +1 to +590 after the *pfap2-hs* STOP codon. It was cloned into *Xho*I-*Aat*II restriction sites. The donor plasmid for 3xHA C-terminal tagging (pHR-C_pfap2hs_3xHA_hsp90-3') was also based on plasmid pHRap2g-eYFP[52], with the eYFP coding sequence replaced by the 3xHA sequence (amplified from plasmid pHH1inv-pfap2-g-HAx3[41]) and the same homology regions as in plasmid pHR-C_pfap2hs_eYFP (but HR2 was cloned, using the In-Fusion system, into *EcoR*I-*Aat*II sites, because in this construct the *hsp90* 3' region in pHRap2g-eYFP was maintained).

For N-terminal tagging (10E_*pfap2-hs*_eYFP-Nterm line), we cloned a guide targeting *pfap2-hs* positions 73-92 in the pDC2-Cas9-U6-hDHFRyFCU[53] plasmid to obtain plasmid pDC2_pfap2hs_sgRNA-N (Extended Data Fig. 2d, Supplementary Table 5). The donor plasmid (pfap2hs_HR-N_eYFP) consisted of a 5' homology region (HR1) including positions -366 to -1 relative to the *pfap2-hs* start codon, the eYFP gene and an in frame 3' homology region (HR2) spanning positions 4-756 of the gene (excluding the ATG) in which the nucleotides up to the position of the guide were recodonized. HR1 and HR2 were cloned into *Sac*II-*Nco*I and *Spe*I-*Eco*RI sites, respectively. HR2 was

amplified in two steps using a nested PCR approach to add the recodonized sequences. The eYFP fragment (PCR-amplified from plasmid pHR-C_pfap2hs_eYFP) was cloned using the In-Fusion system into *Spe*I/*Nco*I sites.

To tag PfAP2-HS with a 2xHA-ddFKBP domain tag (1.2B_ *pfap2-hs*_ddFKBP line) we used a single homologous recombination approach (Extended Data Fig. 2e). To generate the pfap2hs_HA-ddFKBP plasmid, we replaced the *pfap2-g* homology region in plasmid PfAP2-G-ddFKBP[41] by a PCR-amplified fragment including positions 9,551-11,574 of *pfap2-hs* in frame with the tag. The fragment was cloned using restriction sites *Not*I and *Xho*I. All oligonucleotides used to generate the plasmids are described in Supplementary Table 5. The relevant parts of all plasmids (i.e., the new sequences incorporated) were sequenced before transfection.

Transfections were performed by electroporation of ring stage cultures with 100 µg of plasmid (HA-ddFKBP tagging) or with a mixture of 12 µg linearized donor plasmid and 60 µg of circular Cas9 plasmid (CRISPR-Cas9 system). Linearization was achieved by digestion with the *Pvu*I restriction enzyme (cleaving the *amp* resistance gene of the donor plasmid). Transfected cultures were selected with 10 nM WR99210 for four days as previously described[53] (transfections using the CRISPR-Cas9 system), or with continuous WR99210 pressure until parasites were observed, followed by 3 off/on drug cycles and subcloning by limiting dilution (transfections with the pfap2hs_HA-ddFKBP plasmid). In all cases, to assess correct integration we used analytical PCR of

genomic DNA (Extended Data Fig. 2) with specific primers (Supplementary Table 5).

Heat-shock resistance assay. Heat-shock was always performed on cultures at the mature trophozoite stage unless otherwise indicated. To measure survival to heat-shock, cultures were tightly synchronized to a defined age window, diluted to 1% parasitaemia, split in two identical petri dishes (heat-shock and control) maintained in independent air-tight incubation chambers, and exposed to heat-shock when the majority of parasites were at the mature trophozoite stage (typically ~30-35 h post-invasion, hpi; Δ*pfap2-hs* lines were tightly synchronized 3 h earlier than the other lines but exposed to heat-shock in parallel to account for their slower IDC progression). The exception was experiments to screen many subclones (i.e., Fig. 1f) or to characterize transgenic parasite lines (i.e., Extended Data Fig. 2), in which cultures were only sorbitol-synchronized and heat-shock performed ~20-25 h after sorbitol lysis (mature trophozoite stage). For heat-shock, the full incubation chamber was transferred to an incubator at 41.5ºC for 3 h, and then placed back to 37 or 35ºC (the latter temperature was used for all lines in experiments including the *pfap2-hs* knockout lines). The chamber with the control cultures was always maintained at 37 or 35ºC. After reinvasion (typically ~60-70 h after synchronization to ensure that all parasites had completed the cycle, including parasites subjected to heat-shock that show delayed progression through the IDC), parasitaemia of control and heat-shock-exposed cultures was measured by flow cytometry using a FACScalibur flow cytometer (Becton Dickinson) and

SYTO 11 to stain nucleic acids (Supplementary Fig. 1), as previously described[54].

Phenotypic characterization. To determine the growth rate (increase in parasitaemia between consecutive cycles) at different temperatures, the parasitaemia of sorbitol-synchronized cultures was adjusted to 1% and then accurately determined by flow cytometry. Cultures where then split between two or three dishes maintained in parallel in incubators at the different temperatures tested. Parasitaemia was again determined by flow cytometry at the next cycle to determine the growth rate. To measure the duration of the IDC (at 35ºC) in the different parasite lines we used a recently described method based on synchronization to a 1 h age window achieved by Percoll-purification of schizonts followed by sorbitol lysis 1 h later[54]. The determination of the number of merozoites per fully mature schizont was based on light microscopy analysis of Giemsa-stained smears from Percoll-purified schizonts[54]. DHA (Sigma no. D7439) or epoxomicin (Selleckchem no. S7038) sensitivity was measured after exposing tightly synchronized cultures (1% parasitaemia) at the ring (10-15 hpi, DHA only) or trophozoite (30-35 hpi, DHA or epoxomicin) stage to a 3 h pulse of the compounds at different concentrations (DHA, 2.5, 5, 10, 20 or 200 nM, which is lower than the ~700 nM plasma concentration after patient treatment that kills the vast majority of sensitive parasites[35]; epoxomicin, 100 or 150 nM, which is higher than the reported 7.7 nM IC_{50} after exposing parasites for 50 h[55] and similar to the concentration used in previous studies with a 3 h pulse[29,38]). Parasitaemia was measured by light microscopy analysis of Giemsa-stained smears at the next cycle (typically 70-80 h after Percoll-sorbitol

synchronization). For these experiments, the Δ*pfap2-hs* lines were tightly synchronized 3 h earlier than the other lines but exposed to DHA or epoxomicin in parallel (13-18 or 33-38 hpi), to account for their slower IDC progression. For DHA experiments, drug concentrations were log transformed and percent survival data were fit to sigmoidal dose-response curves to calculate the IC_{50} values using GraphPad Prism.

Transcriptional analysis by RT-qPCR. RNA from tightly synchronized cultures exposed to heat-shock and their controls was obtained using the Trizol method, DNAse-treated and purified essentially as described. Reverse transcription and qPCR analysis of cDNAs were also performed as described before[56,57]. In brief, a mixture of random primers and oligo (dT) were used for reverse transcription, and for qPCR we used the PowerSYBR Green Master Mix (Applied biosystems) and the standard curve method (each plate included a standard curve for each primer pair). All primers used are listed in Supplementary Table 5. Unless otherwise indicated, transcript levels were normalized against *serine--tRNA ligase* (PF3D7_0717700), which shows relatively stable expression throughout the IDC.

Transcriptomic analysis using microarrays. To compare the transcriptome of control and heat-shock-adapted 3D7-A parasite lines across the IDC we used previously described two-colour long oligonucleotide-based glass microarrays[21]. RNA was obtained from tightly synchronized cultures (5 h age window) at 8-13, 16-21, 24-29, 32-37 and 40-45 hpi. All samples (Cy5-labeled) were hybridized together with a reference pool (Cy3-labeled) consisting of a mixture of equal

amounts of cDNA from rings, trophozoites and schizonts from control and heat-shock-adapted lines. Comparative genome hybridization was used to identify potential transcript level differences attributable to genetic deletions or duplications. 5,142 genes produced useful data. Sample preparation, microarray hybridization and data analysis were performed essentially as described[21].

To analyse the transcriptome of 10E, 10G and 10E_Δ*pfap2-hs* parasite lines under control and heat-shock conditions, we used two-colour long oligonucleotide-based custom Agilent microarrays[58]. The microarray design was based on Agilent design AMADID no. 037237[58,59], but we modified it as previously described (new design AMADID no. 084561)[60]. RNA was obtained from cultures synchronized to a 5 h age window at a ~2.5% parasitaemia. Given the slower IDC progression of 10E_Δ*pfap2-hs*, cultures of this parasite line were synchronized to 0-5 hpi 3 h earlier than 10E and 10G cultures, such that at the time of starting heat-shock (in parallel for all lines) all cultures were approximately at the same stage of IDC progression. Heat-shock was started at 30-35 hpi (33-38 hpi for the 10E_Δ*pfap2-hs* line) and samples collected before, during and after heat-shock as indicated. RNA was prepared using the Trizol method. Sample preparation and microarray hybridization were performed essentially as described[59]. All samples (Cy5-labeled) were hybridized together with a reference pool (Cy3-labeled) consisting of a mixture of equal amounts of cDNA from rings, trophozoites and schizonts from 3D7-A. Microarray images were obtained using a DNA Microarray Scanner (no. G2505C, Agilent Technologies) located in a low ozone area, and initial data processing was

performed using the GE2 _1105_Oct12 extraction protocol in Agilent Feature Extraction 11.5.1.1 software.

Agilent microarray data was analysed using Bioconductor in an R environment (R version 3.5.3). For each individual microarray, we calculated Cy3 and Cy5 background signal as the median of the 100 lowest signal probes for each channel, and probes with both Cy3 and Cy5 signals below three times the array background were excluded. Gene level $\log_2$(Cy5/Cy3) values, statistical estimation of parasite age[61] and estimation of average expression fold-differences across a time interval (for the comparison between parasite lines in the absence of heat-shock) were performed as described[21]. The $\log_2$ of the expression fold-change upon heat-shock was calculated, for each gene and time point, as the $\log_2$(Cy5/Cy3) in the heat-shock-exposed sample minus the $\log_2$(Cy5/Cy3) in the control sample at the same parasite age, calculated using linear interpolation in the $\log_2$(Cy5/Cy3) versus estimated age plot. Visual inspection was used to exclude from further analysis genes with apparent artefacts. Genes missing data for ≥2 time points (or ≥1 for the comparison between parasite lines in the absence of heat-shock across a time interval), or with values within the lowest 15th percentile of expression intensity (Cy5 sample channel) in all samples, were also excluded from further analysis. 4,964 genes produced useful data.

To assess the level of similarity between the transcriptome of our samples and a reference non-stressed transcriptome with high temporal resolution (HB3 line)[28] we calculated the Pearson correlation between each sample and the time

point of the reference transcriptome with which it has higher similarity. Heatmaps and hierarchical clustering based on Spearman (Fig. 2) or Pearson (Extended Data Fig. 6) correlation were generated using Multiple Experiment Viewer (MeV) 4.9[62]. Expression trend plots for each cluster were generated using ggplot2, with LOESS smoothing, and Venn diagrams using the eulerr package (both in an R environment). Motif analysis (5 to 8 bp) was performed using MEME 5.0.3 software. Functional enrichment analysis using GO terms annotated in PlasmoDB release 43 was performed using Ontologizer 2.1 software[63] with the topology-elim method[64]. Gene set enrichment analysis (GSEA) was performed using GSEA v3.0 Preranked[65].

Whole-genome sequencing analysis, analysis of publicly available genome sequences from field isolates and phylogenetic analysis. To sequence the full genome of control and heat-shock-adapted 3D7-A lines (two biological replicates), we used PCR-free whole-genome Illumina sequencing. In brief, genomic DNA was sheared to ~150-400 bp fragments using a Covaris S220 ultrasonicator and analysed using an Agilent 2100 Bioanalyzer. For library preparation we used the NEBNext DNA Library Prep Master Mix Set for Illumina (no. E6040S) using specific paired-end TruSeq Illumina adaptors for each sample. After quality check by qPCR, we obtained >6 million 150 bp paired reads for each sample using an Illumina MiSeq sequencing system. After checking reads quality (FastQC algorithm) and trimming adaptors (Cutadapt algorithm), sequence reads were mapped to the PlasmodDB *P. falciparum* 3D7 reference genome release 24 (https://plasmodb.org/plasmo/) using the Bowtie2 local alignment algorithm and alignment quality was assessed using the

621 QualiMap platform. Average genome coverage was 76 to 98-fold. To identify
622 SNPs and small indels we followed the Genome Analysis Toolkit (GATK) best
623 practices workflow, using SAMtools, PicardTools and GATK algorithms. Variant
624 calling was performed using GATK-UnifiedGenotyper. Variants with low calling
625 quality (Phred QUAL<20) and low read depth (DP<10) were filtered out using
626 GATK-VariantFiltration, and only variants present in both biological replicates
627 were considered. Differences in SNP/indel frequency between control and heat-
628 shock-adapted lines were calculated for each SNP/indel using Microsoft Excel,
629 and those showing <25% difference in any of the two replicates were filtered
630 out. Genome Browse (Golden Helix) was used to visualize alignments and
631 variants.
632
633 For the analysis of publicly available genome sequences, we used the Pf3K
634 Project (2016): pilot data release 5 (www.malariagen.net/data/pf3k-5) containing
635 the sequence of >2,500 field isolates. Only SNPs that passed all quality filters
636 and did not fall within a region with multiple large insertions and deletions were
637 considered to be high-confidence. Using these criteria, a single high-confidence
638 polymorphism (occurring in a single isolate) was identified at the *pfap2-hs* gene
639 (producing the C3168X mutation that results in a truncated PfAP2-HS protein
640 that lacks D3).
641
642 For sequence alignment and construction of the phylogenetic tree (with the
643 Neighbor-Joining method) we used Clustal Omega[66], with default parameters.
644 From the tree without distance corrections obtained, the cladogram was
645 generated using FigTree 1.4.4.

ChIP experiments and data analysis. For ChIP experiments, synchronous 50 ml cultures at 2.5 to 5% parasitemia were harvested at the mid trophozoite stage. For replicates in which ChIP was performed in parallel under heat-shock and control conditions, cultures were split off from a single parent flask at the mid trophozoite stage. Control flasks were immediately returned to 37ºC whereas heat-shock flasks were maintained at 41.5ºC for 3 h before harvesting for ChIP analysis.

ChIP followed by qPCR or Illumina sequencing was performed as described[67] using the 3F10 rat anti-HA antibody (1:500; Roche no. 11867423001) to immunoprecipitate HA tagged AP2-HS, with the following modification: total chromatin was diluted 5-fold in dilution buffer following sonication. The Illumina HiSeq system was used to obtain 125 bp paired-end (replicates 1-3) or 150 bp single-end (replicates 4-5) reads.

ChIP-seq data analysis was performed essentially as described[67]. In brief, after trimming, quality control, mapping the remaining reads to the *Plasmodium falciparum* genome (PlasmoDB release 28) using BWA-MEM and filtering duplicated reads, peak calling was performed using MACS2[68] with a q-value cut-off of 0.01. Conversion to $\log_2$ coverage of immunoprecipitate/input was performed using DeepTools BamCompare, selecting the paired end parameter for all tools when analyzing experiments including control and heat-shock conditions. Overlapping intervals within called peaks for each dataset were determined using Bedtools MultiIntersect. The closest annotated gene coding

sequence for each called peak was determined using Bedtools ClosestBed. To visualize aligned data, we used the Integrative Genomics Viewer (IGV).

ChIP samples were analysed by qPCR in triplicate wells with primers described in Supplementary Table 5. All primer pairs were confirmed to have between 80 and 110% efficiency using sheared genomic DNA as a template control. The percent input was calculated using the formula $100*2^{(Ct\ adjusted\ input - Ct\ IP)}$.

Western blot. Synchronized cultures at the mature trophozoite stage were exposed to a regular 3 h heat-shock or to a 1.5 h DHA pulse (10 or 100 nM, used as positive control for a condition known to produce proteotoxic stress and induce the UPR)[29,38]. Parasites were obtained using saponin lysis (0.15% w/v saponin) and pellets solubilized in 1x SDS-PAGE loading buffer with 4% β-mercaptoethanol and boiled at 95ºC for 5 min. Proteins were resolved by SDS-PAGE on 4-20% TGX Mini-PROTEAN gels (Bio-rad) and transferred to nitrocellulose membranes (Bio-rad). After blocking with 5% (w/v) bovine serum albumin (Biowest) in TBS-T (0.1% Tween 20 in tris buffered saline), membranes were incubated at 4ºC overnight with the following primary antibodies: rabbit anti-ubiquitin (1:1,000; Cell Signaling Technology no. 3933), rabbit anti-phospho-eIF2α (1:1,000; Cell Signaling Technology no. 3398) and rabbit anti-histone H3 (1:1,000; Cell Signaling Technology no. 9715). After incubation with a goat anti-rabbit IgG-peroxidase (1:5,000; Millipore no. AP307P) secondary antibody, peroxidase was detected using the Pierce ECL Western Blotting Substrate (Thermo Fisher Scientific) in an ImageQuant LAS 4000 imaging system. To control for equal loading, parts of the membranes corresponding to

different molecular weight ranges were separately hybridized with different antibodies. Signal quantification was performed using ImageJ.

Statistical analysis. Statistical analysis was performed using Microsoft Excel and GraphPad Prism. *P* values were calculated using a two-tailed *t*-test (equal variance). No adjustment for multiple comparisons was made. Only significant *P* values ($P<0.05$) are shown in the figures. No statistical analysis was performed for experiments involving only two replicates. In all cases, *n* indicates independent biological replicates (i.e., samples were obtained from independent cultures).

Code availability. The scripts used for the analysis of microarray and next generation sequencing data are available at github (https://github.com/CortesMalariaLab/PfAP2-HS_Tinto_etal_NatMicrobiol_2021, with doi: 10.5281/zenodo.4775988).

Data availability. The microarray data presented in Fig. 2 and Extended Data Fig. 1, 5, 6 and 8 has been deposited to the Gene Expression Omnibus (GEO) database with accession code GSE149394. Genome sequencing and ChIP-seq data presented in Fig. 1b, Fig. 2e and Extended Data Fig. 7 have been deposited to the Sequence Read Archive (SRA) database with accession codes PRJNA626524 and PRJNA670721, respectively. The authors declare that all other relevant data generated or analysed during this study are included in the Article, the Extended Data or the Supplementary Information files. Source data is provided with this Article. We used data from the Pf3k pilot data release 5

(www.malariagen.net/pf3k) and different releases of PlasmoDB (www.plasmodb.org) databases. Materials described in this article, including the *P. falciparum* transgenic lines, are available from the corresponding author on reasonable request.

REFERENCES

1 Richter, K., Haslbeck, M. & Buchner, J. The heat shock response: life on the verge of death. *Mol Cell* **40**, 253-266 (2010).

2 Hartl, F. U., Bracher, A. & Hayer-Hartl, M. Molecular chaperones in protein folding and proteostasis. *Nature* **475**, 324-332 (2011).

3 Anckar, J. & Sistonen, L. Regulation of HSF1 function in the heat stress response: implications in aging and disease. *Annu Rev Biochem* **80**, 1089-1115 (2011).

4 Mahat, D. B., Salamanca, H. H., Duarte, F. M., Danko, C. G. & Lis, J. T. Mammalian Heat Shock Response and Mechanisms Underlying Its Genome-wide Transcriptional Regulation. *Mol Cell* **62**, 63-78 (2016).

5 Solis, E. J. *et al.* Defining the Essential Function of Yeast Hsf1 Reveals a Compact Transcriptional Program for Maintaining Eukaryotic Proteostasis. *Mol Cell* **63**, 60-71 (2016).

6 Gomez-Pastor, R., Burchfiel, E. T. & Thiele, D. J. Regulation of heat shock transcription factors and their roles in physiology and disease. *Nat Rev Mol Cell Biol* **19**, 4-19 (2018).

7 Milner, D. A., Jr. Malaria Pathogenesis. *Cold Spring Harb Perspect Med* **8**, a025569 (2018).

8 Kwiatkowski, D. Malarial toxins and the regulation of parasite density. *Parasitol Today* **11**, 206-212 (1995).

9 Oakley, M. S., Gerald, N., McCutchan, T. F., Aravind, L. & Kumar, S. Clinical and molecular aspects of malaria fever. *Trends Parasitol* **27**, 442-449 (2011).

10 Gravenor, M. B. & Kwiatkowski, D. An analysis of the temperature effects of fever on the intra-host population dynamics of *Plasmodium falciparum*. *Parasitology* **117 (Pt 2)**, 97-105 (1998).

11 Kwiatkowski, D. Febrile temperatures can synchronize the growth of *Plasmodium falciparum* in vitro. *J Exp Med* **169**, 357-361 (1989).

12 Long, H. Y., Lell, B., Dietz, K. & Kremsner, P. G. *Plasmodium falciparum*: in vitro growth inhibition by febrile temperatures. *Parasitol Res* **87**, 553-555 (2001).

13 Portugaliza, H. P. *et al.* Artemisinin exposure at the ring or trophozoite stage impacts *Plasmodium falciparum* sexual conversion differently. *Elife* **9**, e60058 (2020).

14 Pavithra, S. R., Kumar, R. & Tatu, U. Systems analysis of chaperone networks in the malarial parasite *Plasmodium falciparum*. *PLoS Comput Biol* **3**, e168 (2007).

15 Muralidharan, V., Oksman, A., Pal, P., Lindquist, S. & Goldberg, D. E. *Plasmodium falciparum* heat shock protein 110 stabilizes the asparagine repeat-rich parasite proteome during malarial fevers. *Nat Commun* **3**, 1310 (2012).

16 Silva, M. D. *et al.* A role for the *Plasmodium falciparum* RESA protein in resistance against heat shock demonstrated using gene disruption. *Mol Microbiol* **56**, 990-1003 (2005).
17 Kudyba, H. M. *et al.* The endoplasmic reticulum chaperone PfGRP170 is essential for asexual development and is linked to stress response in malaria parasites. *Cell Microbiol* **21**, e13042 (2019).
18 Lu, K. Y. *et al.* Phosphatidylinositol 3-phosphate and Hsp70 protect *Plasmodium falciparum* from heat-induced cell death. *Elife* **9** (2020).
19 Zhang, M. *et al.* The endosymbiotic origins of the apicoplast link fever-survival and artemisinin-resistance in the malaria parasite. *BioRxiv (pre-review preprint)* **doi: https://doi.org/10.1101/2020.12.10.419788**.
20 Oakley, M. S. *et al.* Molecular factors and biochemical pathways induced by febrile temperature in intraerythrocytic *Plasmodium falciparum* parasites. *Infect Immun* **75**, 2012-2025 (2007).
21 Rovira-Graells, N. *et al.* Transcriptional variation in the malaria parasite *Plasmodium falciparum*. *Genome Res* **22**, 925-938 (2012).
22 Balaji, S., Babu, M. M., Iyer, L. M. & Aravind, L. Discovery of the principal specific transcription factors of Apicomplexa and their implication for the evolution of the AP2-integrase DNA binding domains. *Nucleic Acids Res* **33**, 3994-4006 (2005).
23 Campbell, T. L., De Silva, E. K., Olszewski, K. L., Elemento, O. & Llinas, M. Identification and genome-wide prediction of DNA binding specificities for the ApiAP2 family of regulators from the malaria parasite. *PLoS Pathog* **6**, e1001165 (2010).
24 Jeninga, M. D., Quinn, J. E. & Petter, M. ApiAP2 Transcription Factors in Apicomplexan Parasites. *Pathogens* **8**, E47 (2019).
25 Militello, K. T., Dodge, M., Bethke, L. & Wirth, D. F. Identification of regulatory elements in the *Plasmodium falciparum* genome. *Mol Biochem Parasitol* **134**, 75-88 (2004).
26 Dobson, C. M., Sali, A. & Karplus, M. Protein Folding: A Perspective from Theory and Experiment. *Angew Chem Int Ed Engl* **37**, 868-893 (1998).
27 Masterton, R. J., Roobol, A., Al-Fageeh, M. B., Carden, M. J. & Smales, C. M. Post-translational events of a model reporter protein proceed with higher fidelity and accuracy upon mild hypothermic culturing of Chinese hamster ovary cells. *Biotechnol Bioeng* **105**, 215-220 (2010).
28 Bozdech, Z. *et al.* The Transcriptome of the Intraerythrocytic Developmental Cycle of *Plasmodium falciparum*. *PLoS Biol* **1**, E5 (2003).
29 Dogovski, C. *et al.* Targeting the cell stress response of *Plasmodium falciparum* to overcome artemisinin resistance. *PLoS Biol* **13**, e1002132 (2015).
30 Claessens, A., Affara, M., Assefa, S. A., Kwiatkowski, D. P. & Conway, D. J. Culture adaptation of malaria parasites selects for convergent loss-of-function mutants. *Sci Rep* **7**, 41303 (2017).
31 Stewart, L. B. *et al.* Intrinsic multiplication rate variation and plasticity of human blood stage malaria parasites. *Commun Biol* **3**, 624 (2020).
32 Manske, M. *et al.* Analysis of *Plasmodium falciparum* diversity in natural infections by deep sequencing. *Nature* **487**, 375-379 (2012).
33 Lamech, L. T. & Haynes, C. M. The unpredictability of prolonged activation of stress response pathways. *J Cell Biol* **209**, 781-787 (2015).
34 Blasco, B., Leroy, D. & Fidock, D. A. Antimalarial drug resistance: linking *Plasmodium falciparum* parasite biology to the clinic. *Nat Med* **23**, 917-928 (2017).
35 Haldar, K., Bhattacharjee, S. & Safeukui, I. Drug resistance in *Plasmodium*. *Nat Rev Microbiol* **16**, 156-170 (2018).
36 Ariey, F. *et al.* A molecular marker of artemisinin-resistant *Plasmodium falciparum* malaria. *Nature* **505**, 50-55 (2014).

37 Birnbaum, J. *et al.* A Kelch13-defined endocytosis pathway mediates artemisinin resistance in malaria parasites. *Science* **367**, 51-59 (2020).
38 Bridgford, J. L. *et al.* Artemisinin kills malaria parasites by damaging proteins and inhibiting the proteasome. *Nat Commun* **9**, 3801 (2018).
39 Mok, S. *et al.* Drug resistance. Population transcriptomics of human malaria parasites reveals the mechanism of artemisinin resistance. *Science* **347**, 431-435 (2015).
40 Lindner, S. E., De Silva, E. K., Keck, J. L. & Llinas, M. Structural Determinants of DNA Binding by a *P. falciparum* ApiAP2 Transcriptional Regulator. *J Mol Biol* **395**, 558-567 (2010).
41 Kafsack, B. F. *et al.* A transcriptional switch underlies commitment to sexual development in malaria parasites. *Nature* **507**, 248-252 (2014).
42 Modrzynska, K. *et al.* A Knockout Screen of ApiAP2 Genes Reveals Networks of Interacting Transcriptional Regulators Controlling the *Plasmodium* Life Cycle. *Cell Host Microbe* **21**, 11-22 (2017).
43 Zhang, C. *et al.* Systematic CRISPR-Cas9-Mediated Modifications of *Plasmodium yoelii* ApiAP2 Genes Reveal Functional Insights into Parasite Development. *mBio* **8** (2017).
44 Llora-Batlle, O., Tinto-Font, E. & Cortes, A. Transcriptional variation in malaria parasites: why and how. *Brief Funct Genomics* **18**, 329-341 (2019).

References cited only in the Methods section.

45 Cortés, A., Benet, A., Cooke, B. M., Barnwell, J. W. & Reeder, J. C. Ability of *Plasmodium falciparum* to invade Southeast Asian ovalocytes varies between parasite lines. *Blood* **104**, 2961-2966 (2004).
46 Cortés, A. A chimeric *Plasmodium falciparum Pfnbp2b*/*Pfnbp2a* gene originated during asexual growth. *Int J Parasitol* **35**, 125-130 (2005).
47 Cortés, A. *et al.* Epigenetic silencing of *Plasmodium falciparum* genes linked to erythrocyte invasion. *PLoS Pathog* **3**, e107 (2007).
48 Walliker, D. *et al.* Genetic analysis of the human malaria parasite *Plasmodium falciparum*. *Science* **236**, 1661-1666 (1987).
49 Anders, R. F., Brown, G. V. & Edwards, A. Characterization of an S antigen synthesized by several isolates of *Plasmodium falciparum*. *Proc Natl Acad Sci USA* **80**, 6652-6656 (1983).
50 Ghorbal, M. *et al.* Genome editing in the human malaria parasite *Plasmodium falciparum* using the CRISPR-Cas9 system. *Nat Biotechnol* **32**, 819-821 (2014).
51 Lim, M. Y. *et al.* UDP-galactose and acetyl-CoA transporters as *Plasmodium* multidrug resistance genes. *Nat Microbiol* **1**, 16166 (2016).
52 Bancells, C. *et al.* Revisiting the initial steps of sexual development in the malaria parasite *Plasmodium falciparum*. *Nat Microbiol* **4**, 144-154 (2019).
53 Knuepfer, E., Napiorkowska, M., van Ooij, C. & Holder, A. A. Generating conditional gene knockouts in *Plasmodium* - a toolkit to produce stable DiCre recombinase-expressing parasite lines using CRISPR/Cas9. *Sci Rep* **7**, 3881 (2017).
54 Rovira-Graells, N., Aguilera-Simon, S., Tinto-Font, E. & Cortes, A. New Assays to Characterise Growth-Related Phenotypes of *Plasmodium falciparum* Reveal Variation in Density-Dependent Growth Inhibition between Parasite Lines. *PLoS ONE* **11**, e0165358 (2016).
55 Prasad, R. *et al.* Blocking *Plasmodium falciparum* development via dual inhibition of hemoglobin degradation and the ubiquitin proteasome system by MG132. *PLoS One* **8**, e73530 (2013).
56 Crowley, V. M., Rovira-Graells, N., de Pouplana, L. R. & Cortés, A. Heterochromatin formation in bistable chromatin domains controls the

epigenetic repression of clonally variant *Plasmodium falciparum* genes linked to erythrocyte invasion. *Mol Microbiol* **80**, 391-406 (2011).
57 Casas-Vila, N., Pickford, A. K., Portugaliza, H. P., Tintó-Font, E. & Cortés, A. Transcriptional analysis of tightly synchronized *Plasmodium falciparum* intraerythrocytic stages by RT-qPCR. *Methods Mol Biol*, **in press**.
58 Kafsack, B. F., Painter, H. J. & Llinas, M. New Agilent platform DNA microarrays for transcriptome analysis of *Plasmodium falciparum* and *Plasmodium berghei* for the malaria research community. *Malar J* **11**, 187 (2012).
59 Painter, H. J., Altenhofen, L. M., Kafsack, B. F. & Llinas, M. Whole-genome analysis of *Plasmodium* spp. utilizing a new agilent technologies DNA microarray platform. *Methods Mol Biol* **923**, 213-219 (2013).
60 Llorà-Batlle, O. *et al.* Conditional expression of PfAP2-G for controlled massive sexual conversion in *Plasmodium falciparum*. *Sci Adv* **6**, eaaz5057 (2020).
61 Lemieux, J. E. *et al.* Statistical estimation of cell-cycle progression and lineage commitment in *Plasmodium falciparum* reveals a homogeneous pattern of transcription in ex vivo culture. *Proc Natl Acad Sci USA* **106**, 7559-7564 (2009).
62 Saeed, A. I. *et al.* TM4 microarray software suite. *Methods Enzymol* **411**, 134-193 (2006).
63 Bauer, S., Grossmann, S., Vingron, M. & Robinson, P. N. Ontologizer 2.0--a multifunctional tool for GO term enrichment analysis and data exploration. *Bioinformatics* **24**, 1650-1651 (2008).
64 Alexa, A., Rahnenfuhrer, J. & Lengauer, T. Improved scoring of functional groups from gene expression data by decorrelating GO graph structure. *Bioinformatics* **22**, 1600-1607 (2006).
65 Subramanian, A. *et al.* Gene set enrichment analysis: a knowledge-based approach for interpreting genome-wide expression profiles. *Proc Natl Acad Sci USA* **102**, 15545-15550 (2005).
66 Sievers, F. *et al.* Fast, scalable generation of high-quality protein multiple sequence alignments using Clustal Omega. *Mol Syst Biol* **7**, 539 (2011).
67 Josling, G. A. *et al.* Dissecting the role of PfAP2-G in malaria gametocytogenesis. *Nat Commun* **11**, 1503 (2020).
68 Zhang, Y. *et al.* Model-based analysis of ChIP-Seq (MACS). *Genome Biol* **9**, R137 (2008).

ACKNOWLEDGMENTS

The authors thank J.J. López-Rubio (University of Montpellier) for plasmid pL6-*egfp*, M. Lee (Wellcome Sanger Institute) for plasmid pDC2-Cas9-U6-hdhfr and E. Knuepfer (The Francis Crick Institute) for plasmid pDC2-Cas9-U6-hDHFRyFCU. The authors also thank O. Llorà-Batlle and C. Sànchez-Guirado (ISGlobal) for assistance with the generation of plasmids used in this study, N. Rovira-Graells (ISGlobal) and A. Gupta. (Nanyang Technological University) for assistance with 3D7-A and 3D7-A-HS microarray experiments, O. Billker

(Wellcome Sanger Institute) for experiments attempted in *P. berghei* and H. Ginsburg (The Hebrew University of Jerusalem) for providing data from the Malaria Parasite Metabolic Pathways. This publication uses data generated by the Pf3k project (www.malariagen.net/pf3k). This work was supported by grants from the Spanish Ministry of Economy and Competitiveness (MINECO)/ Agencia Estatal de Investigación (AEI) (SAF2013-43601-R, SAF2016-76190-R and PID2019-107232RB-I00 to A.C.), co-funded by the European Regional Development Fund (ERDF, European Union), and from NIH/NIAID (1R01 AI125565 to ML). E.T.-F. and L.M.-T. were supported by fellowships from the Spanish Ministry of Economy and Competitiveness (BES-2014-067901 and BES-2017-081079, respectively), co-funded by the European Social Fund (ESF). T.J.R. was supported by a training grant by NIH/NIGMS (T32 GM125592-01). This research is part of ISGlobal's Program on the Molecular Mechanisms of Malaria, which is partially supported by the Fundación Ramón Areces. We acknowledge support from the Spanish Ministry of Science and Innovation through the "Centro de Excelencia Severo Ochoa 2019-2023" Program (CEX2018-000806-S), and support from the Generalitat de Catalunya through the CERCA Program.

AUTHOR CONTRIBUTIONS

E.T.-F. performed all experiments except for those presented in Extended Data Fig. 1, Western blot and ChIP-seq experiments. L.M.-T., E.T.-F., T.J.R. and A.C. performed the bioinformatics analysis. N.C.-V. performed Western blot experiments. T.J.R. performed and M.L. supervised ChIP-seq experiments. Z.B. provided microarray hybridizations for experiments presented in Extended Data

Fig. 1. D.J.C. advised on clinical isolates and provided Line 1 from The Gambia. E.T.-F. and A.C. conceived the project, designed and interpreted the experiments, and wrote the manuscript (with input from all authors and major input from M.L. and D.J.C.).

COMPETING INTERESTS STATEMENT

The authors declare no competing interests.

CORRESPONDENCE

Correspondence and requests for materials should be addressed to A.C. (alfred.cortes@isglobal.org).

FIGURE LEGENDS

Fig 1. Mutations in PfAP2-HS and sensitivity to heat-shock. a, Schematic of the parasite lines used in this study. Colours indicate wild type PfAP2-HS or truncated forms lacking AP2 domain 3 (ΔD3), the three AP2 domains (ΔD1-3), or virtually the full protein (KO). Parasite lines shown with a colour gradient consist of a mixture of individual parasites expressing different versions of the protein. An asterisk indicates a heat-shock (HS) sensitive phenotype, and r1 and r2 are independent replicates of the selection of 3D7-A with periodic heat-shock (3D7-A-HS r1 and r2 are the selected lines, whereas 3D7-A r1 and r2 are controls maintained in parallel at 37ºC). **b**, Proportion of Illumina reads with (Alt) or without (Ref) a nonsense mutation in *pfap2-hs* in two independently selected heat-shock-adapted cultures (3D7-A-HS r1 and r2) and their controls (3D7-A r1 and r2). **c**, Sanger sequencing confirmation of the mutation (in the r1 replicate, representative of r1 and r2). **d**, Schematic of wild-type PfAP2-HS, PfAP2-

HS_ΔD3 and ΔPfAP2-HS. The position of the AP2 domains is indicated (D1-3). **e**, Survival of tightly synchronized cultures exposed to heat-shock at different ages (in h post-invasion, hpi) for two heat-shock-sensitive (3D7-A r2 and 10G) and two heat-shock-resistant (3D7-A-HS r2 and 1.2B) lines (mean of *n*=2 independent biological replicates). **f**, Heat-shock survival at the trophozoite stage of 3D7-A subclones carrying or not the Q3417X mutation (mean of *n*=2 independent biological replicates). **g**, Heat-shock survival of tightly synchronized cultures of parasite lines expressing wild-type or mutated PfAP2-HS. Values are the mean and s.e.m. of *n*=5 (lines of 3D7 origin) or *n*=3 (HB3 and D10 lines) independent biological replicates. *P* values were calculated using a two-sided unpaired *t*-test.

Fig 2. Global transcriptional alterations in parasites exposed to heat-shock. a, Hierarchical clustering of genes with altered transcript levels (≥4 fold-change at any of the time points analysed) during (1.5 and 3 h) or 2 h after finishing (2 h post) heat-shock (HS). Values are the $\log_2$ of the expression fold-change in heat-shock versus control cultures. 13 genes had values out of the range displayed (actual range: -4.78 to +4.93). For each cluster, mean values (with 95% confidence interval) for the genes in the cluster and representative enriched GO terms are shown. Columns at the left indicate annotation as chaperone[14], presence of the G-box[23] or tandem G-box (TdGbox) in the upstream region, and $\log_2$ fold-change after heat-shock in a previous study[20] (Oakley). **b**, Venn diagrams of the genes altered upon heat-shock in the three parasite lines. **c**, Pearson correlation of the genome-wide transcript levels of each culture versus the most similar time point of a high-density time-course

reference transcriptome[28]. **d**, Age progression during the assay, statistically estimated[61] from the transcriptomic data. **e**, ChIP-seq analysis of HA-tagged PfAP2-HS, representative of *n*=5 and *n*=3 independent biological replicates for 35ºC and heat-shock, respectively. The log_2-transformed ChIP/input ratio at the *hsp70-1* and *hsp90* loci is shown. The position of the tandem G-box is indicated.

Fig 3. Phenotypes of parasite lines lacking PfAP2-HS. a, Growth rate of Δ*pfap2-hs* and parental lines of 3D7 genetic background at different temperatures (mean and s.e.m. of *n*=4 independent biological replicates). *P* values were calculated using a two-sided unpaired *t*-test (10E_Δ*pfap2-hs*: 37 vs. 35ºC, $P=2.3 \times 10^{-3}$; 37.5 vs. 35ºC, $P=1.7 \times 10^{-4}$. 10G_Δ*pfap2-hs*: 37 vs. 35ºC, *P*=0.011; 37.5 vs. 35ºC, *P*=0.001). Only significant *P* values (*P*<0.05) are shown. **b**, Same as in panel **a** for parasite lines of HB3 and D10 genetic background (mean and s.e.m. of *n*=4 independent biological replicates). **c**, Number of merozoites per schizont (median and quartiles box with 10-90 percentile whiskers). Values were obtained from 100 schizonts for each parasite line and condition. **d**, Duration of the asexual blood cycle. The cumulative percent of new rings formed at each time point is shown (mean of *n*=2 independent biological replicates).

Fig 4. Characterisation of a cultured-adapted field isolate with mutations in *pfap2-hs*. a, Schematic of wild-type PfAP2-HS and PfAP2-HS_ΔD1-3 occurring in Line 1 from The Gambia after culture adaptation (C to G mutation at codon 931, S931X). The position of the AP2 domains is indicated (D1-3). **b**,

Frequency of the mutation (as determined by Sanger sequencing) in culture-adapted Line 1 before (Pre) and after (Post) performing a heat-shock (HS) at the trophozoite stage and culturing for an additional cycle (mean of *n*=2 independent biological replicates). **c**, Frequency of the mutation during culture at different temperatures. Day 0 is when the frozen stock from The Gambia (culture-adapted for 91 days) was placed back in culture. **d**, Sanger sequencing determination of the presence or absence of the mutation at codon 931 in Line 1 subclones 4E and 1H. **e**, Heat-shock survival of tightly synchronised 4E and 1H cultures (mean and s.e.m. of *n*=4 independent biological replicates). The *P* value was calculated using a two-sided unpaired *t*-test. **f**, Growth rate of 4E and 1H at different temperatures (mean and s.e.m. of *n*=5 independent biological replicates). No significant difference ($P<0.05$) was observed between growth at 35ºC and 37ºC using a two-sided unpaired *t*-test.

Fig 5. Sensitivity of parasites lacking PfAP2-HS to proteotoxic conditions. **a**, Survival (%) after a 3 h dihydroartemisinin (DHA) pulse at the ring or trophozoite (troph.) stage. Values are the mean and s.e.m. of *n*=3 (3D7-A and Line 1 genetic backgrounds) or mean of *n*=2 (HB3 and D10 genetic backgrounds) independent biological replicates. Mean IC_{50} for each line is shown (same colour code as the plots). **b**, Survival (%) after a 3 h epoxomicin pulse at the trophozoite stage. Values are the mean and s.e.m. of *n*=4 (100 nM) or *n*=3 (150 nM) independent biological replicates. In all panels, *P* values were calculated using a two-sided unpaired *t*-test (only for experiments with $n\geq3$). Only significant *P* values ($P<0.05$) are shown.

Fig 6. Model of the *P. falciparum* heat-shock response and phylogenetic analysis of AP2-HS. **a**, The *P. falciparum* heat-shock response involves rapid upregulation of the expression of a very restricted set of chaperones by PfAP2-HS. The PF3D7_1421800 gene (in brackets) shows PfAP2-HS-dependent increased transcript levels upon heat-shock, but PfAP2-HS binding was not detected in its promoter, and it lacks a G-box. The main defects associated with PfAP2-HS deletion or truncation, under heat-shock or basal conditions, are listed. **b**, Phylogenetic analysis of the protein sequence of AP2-HS orthologs in *Plasmodium* spp. **c**, Schematic of the domain structure of AP2-HS orthologs in *Plasmodium* spp. The position of the AP2 domains (D1-3) is based on domains identified in PlasmoDB release 50, except for those marked with an asterisk that were annotated manually based on sequence alignments.

Fig. 1.

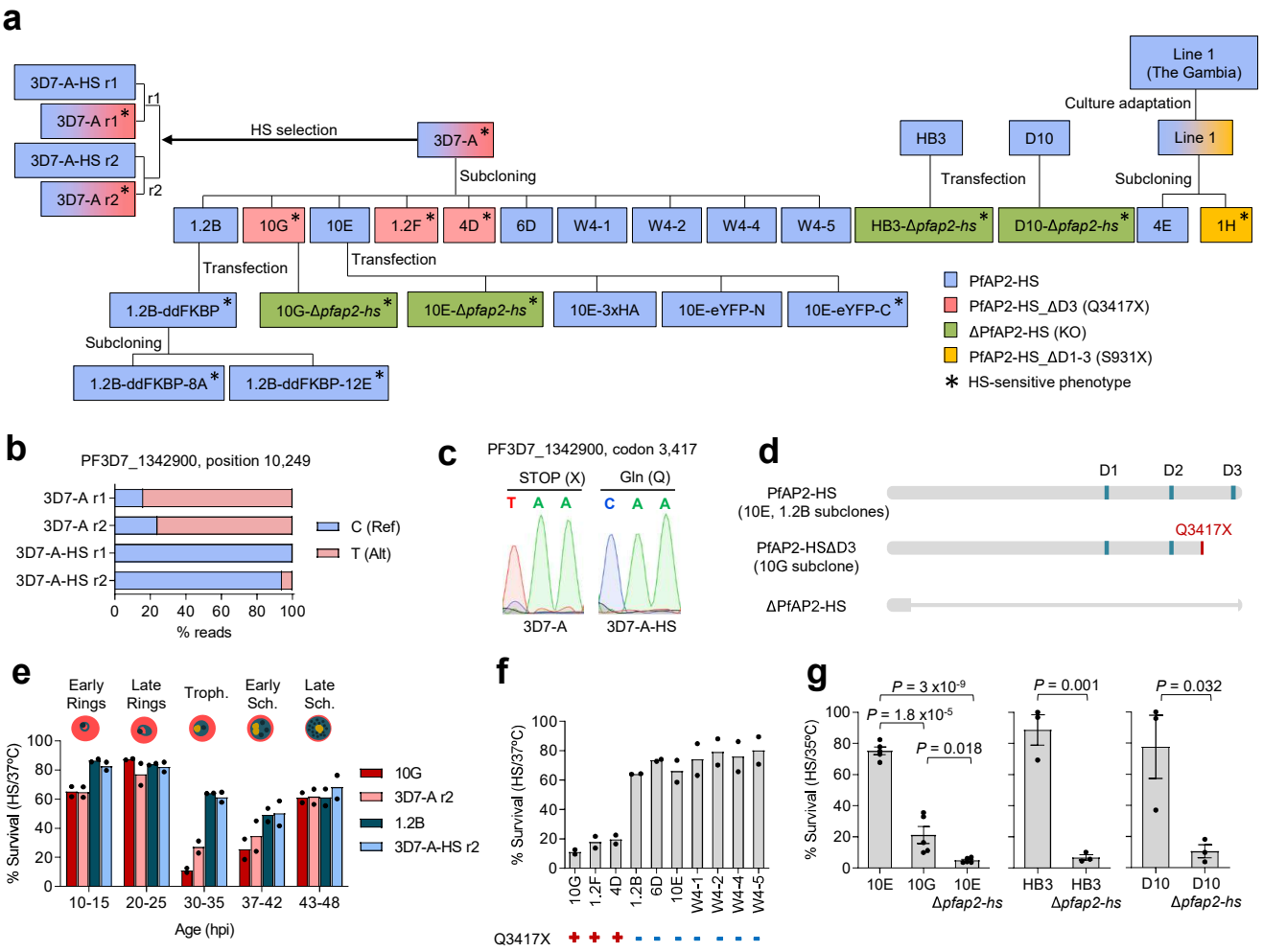
a
3D7-A-HS r1
3D7-A r1 *
r1
3D7-A-HS r2
3D7-A r2 *
r2
HS selection
3D7-A *
Subcloning
1.2B
10G *
10E
1.2F *
4D *
6D
W4-1
W4-2
W4-4
W4-5
Line 1 (The Gambia)
Culture adaptation
Line 1
HB3
D10
Transfection
Subcloning
HB3-Δpfap2-hs *
D10-Δpfap2-hs *
4E
1H *
Transfection
Transfection
1.2B-ddFKBP *
10G-Δpfap2-hs *
10E-Δpfap2-hs *
10E-3xHA
10E-eYFP-N
10E-eYFP-C *
Subcloning
1.2B-ddFKBP-8A *
1.2B-ddFKBP-12E *
PfAP2-HS
PfAP2-HS_ΔD3 (Q3417X)
ΔPfAP2-HS (KO)
PfAP2-HS_ΔD1-3 (S931X)
* HS-sensitive phenotype
b
PF3D7_1342900, position 10,249
3D7-A r1
3D7-A r2
3D7-A-HS r1
3D7-A-HS r2
C (Ref)
T (Alt)
0 20 40 60 80 100
% reads
c
PF3D7_1342900, codon 3,417
STOP (X)
Gln (Q)
T A A
C A A
3D7-A
3D7-A-HS
d
D1 D2 D3
PfAP2-HS (10E, 1.2B subclones)
PfAP2-HSΔD3 (10G subclone)
Q3417X
ΔPfAP2-HS
e
Early Rings
Late Rings
Troph.
Early Sch.
Late Sch.
% Survival (HS/37°C)
10G
3D7-A r2
1.2B
3D7-A-HS r2
10-15
20-25
30-35
37-42
43-48
Age (hpi)
f
% Survival (HS/37°C)
10G 1.2F 4D 1.2B 6D 10E W4-1 W4-2 W4-4 W4-5
Q3417X
g
P = 3 x10-9
P = 1.8 x10-5
P = 0.018
P = 0.001
P = 0.032
% Survival (HS/35°C)
10E 10G 10E
HB3 HB3
D10 D10
Δpfap2-hs

Fig. 2.

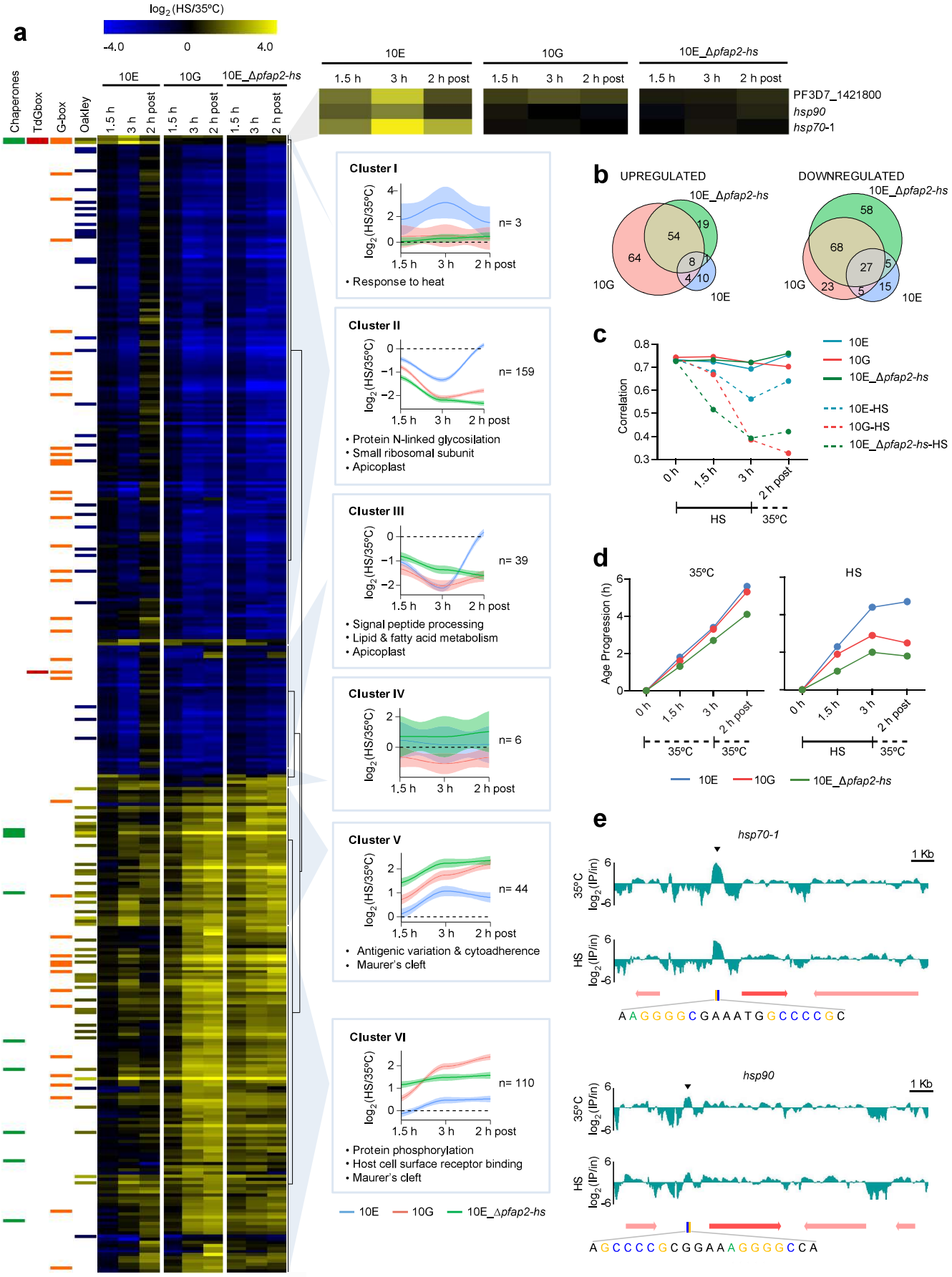
a
log2(HS/35°C)
-4.0
0
4.0
Chaperones
TdGbox
G-box
Oakley
10E
10G
10E_Δpfap2-hs
1.5 h
3 h
2 h post
PF3D7_1421800
hsp90
hsp70-1
Cluster I
n= 3
• Response to heat
Cluster II
n= 159
• Protein N-linked glycosilation
• Small ribosomal subunit
• Apicoplast
Cluster III
n= 39
• Signal peptide processing
• Lipid & fatty acid metabolism
• Apicoplast
Cluster IV
n= 6
Cluster V
n= 44
• Antigenic variation & cytoadherence
• Maurer's cleft
Cluster VI
n= 110
• Protein phosphorylation
• Host cell surface receptor binding
• Maurer's cleft
b
UPREGULATED
DOWNREGULATED
c
Correlation
10E-HS
10G-HS
10E_Δpfap2-hs-HS
HS
35°C
d
Age Progression (h)
e
hsp70-1
hsp90
1 Kb
AAGGGGCGAAATGGCCCCGC
AGCCCCGCGGAAAGGGGCCA

Fig. 3.

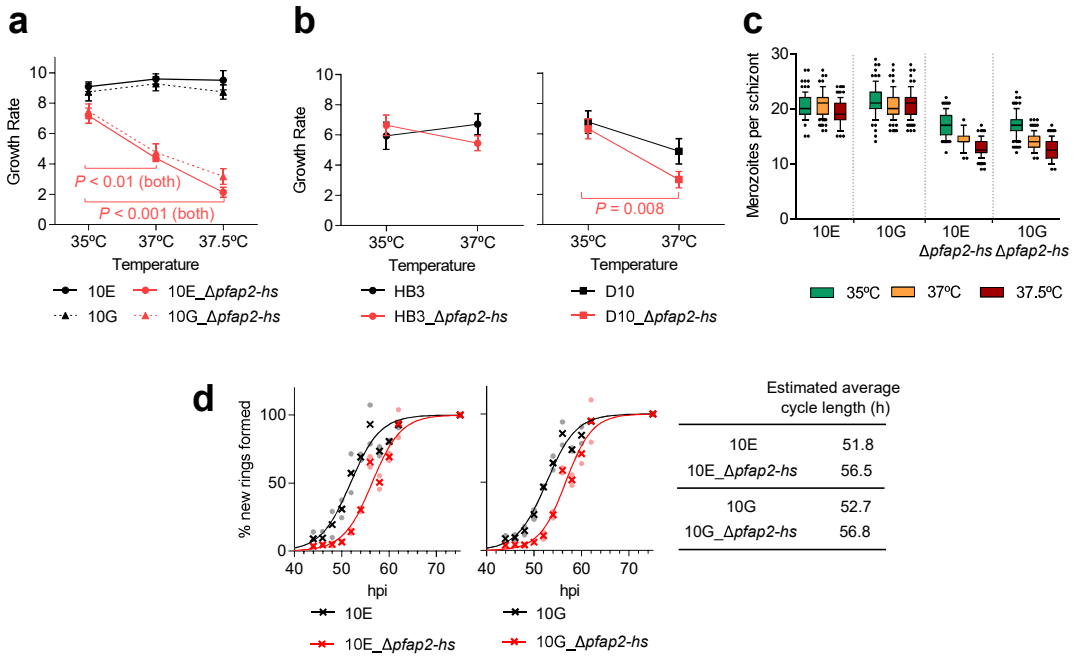

	Estimated average cycle length (h)
10E	51.8
10E_Δ*pfap2-hs*	56.5
10G	52.7
10G_Δ*pfap2-hs*	56.8

Fig. 4.

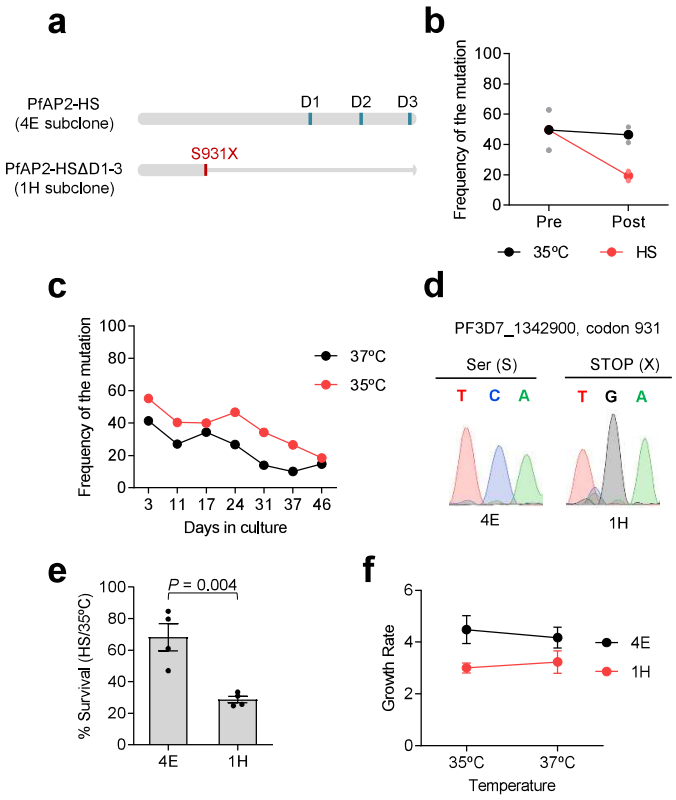
a
PfAP2-HS
(4E subclone)
D1
D2
D3
PfAP2-HSΔD1-3
(1H subclone)
S931X
b
Frequency of the mutation
100
80
60
40
20
0
Pre
Post
35ºC
HS
c
Frequency of the mutation
37ºC
35ºC
3 11 17 24 31 37 46
Days in culture
d
PF3D7_1342900, codon 931
Ser (S)
STOP (X)
T C A
T G A
4E
1H
e
% Survival (HS/35ºC)
P = 0.004
4E
1H
f
Growth Rate
4E
1H
35ºC
37ºC
Temperature

Fig. 5.

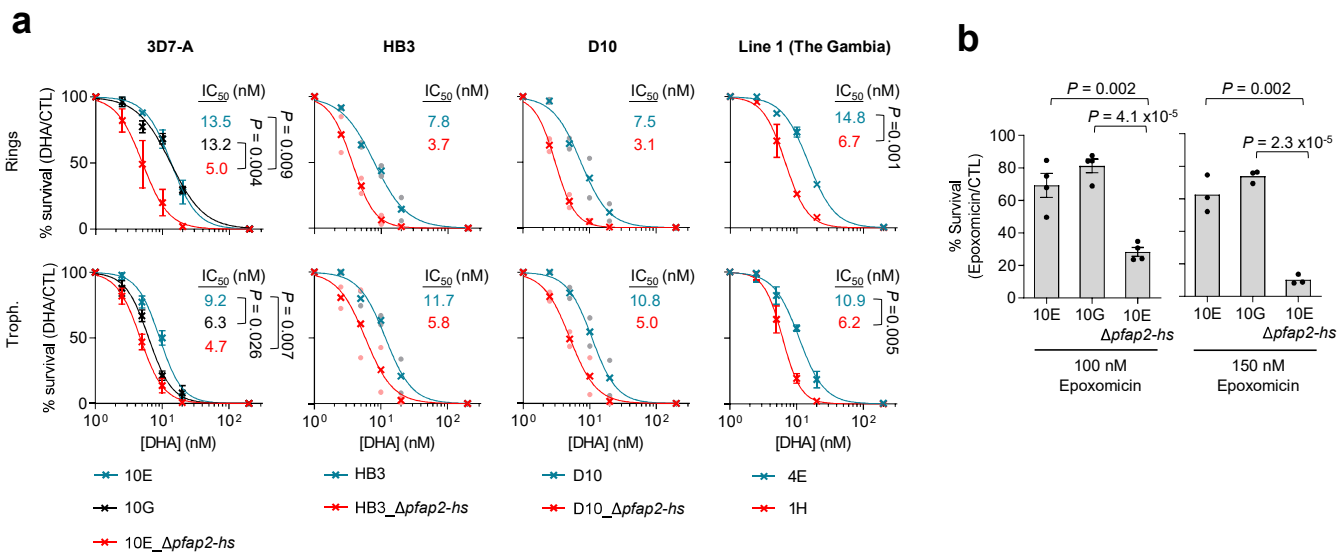
a
3D7-A
HB3
D10
Line 1 (The Gambia)
Rings
Troph.
% survival (DHA/CTL)
IC50 (nM)
13.5
13.2
5.0
P = 0.004
P = 0.009
7.8
3.7
7.5
3.1
14.8
6.7
P = 0.001
9.2
6.3
4.7
P = 0.026
P = 0.007
11.7
5.8
10.8
5.0
10.9
6.2
P = 0.005
[DHA] (nM)
10E
10G
10E_Δpfap2-hs
HB3
HB3_Δpfap2-hs
D10
D10_Δpfap2-hs
4E
1H
b
P = 0.002
P = 4.1 x10-5
P = 0.002
P = 2.3 x10-5
% Survival (Epoxomicin/CTL)
10E
10G
10E Δpfap2-hs
100 nM Epoxomicin
150 nM Epoxomicin

Fig. 6.

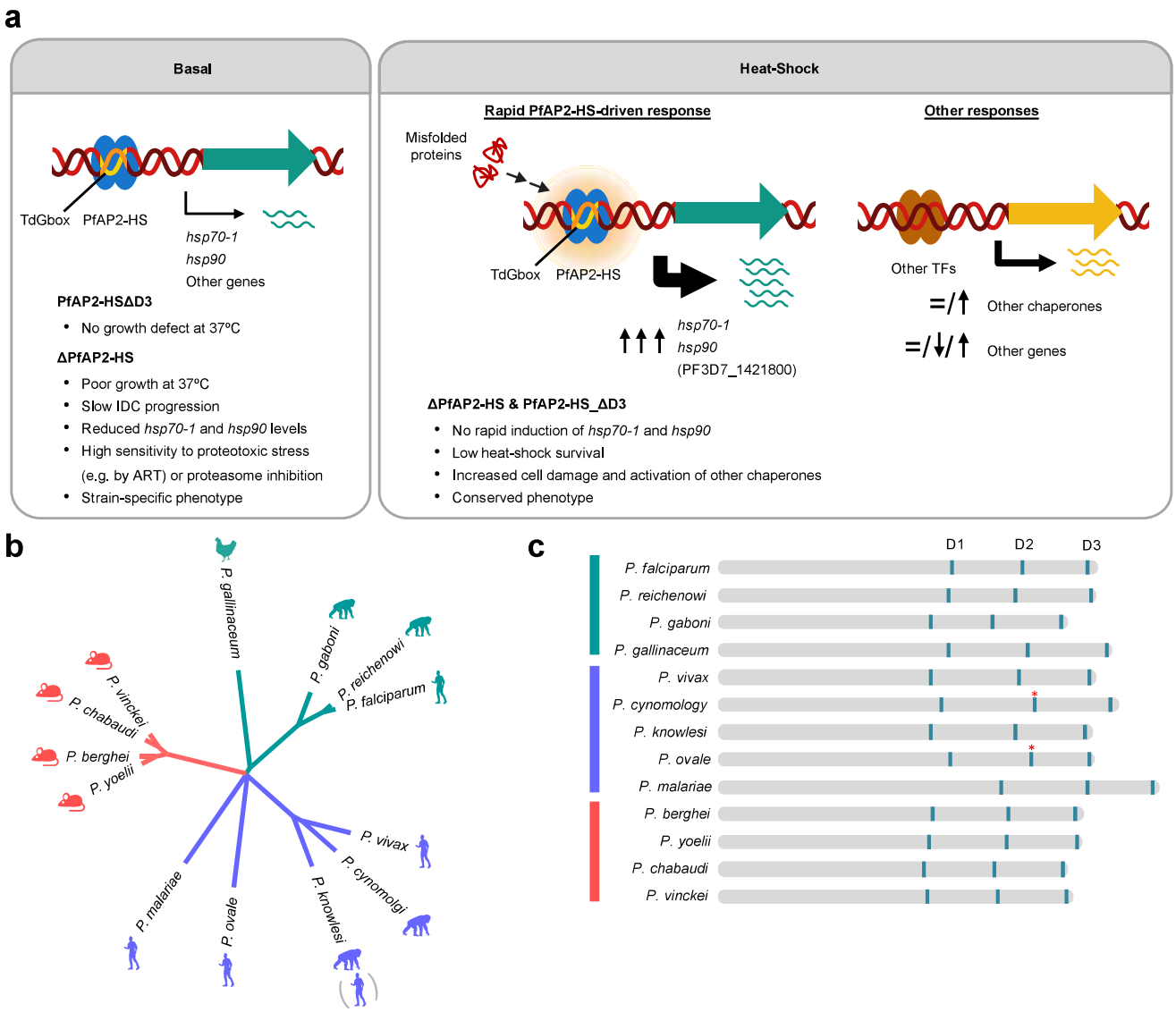
a
Basal
TdGbox
PfAP2-HS
hsp70-1
hsp90
Other genes
PfAP2-HSΔD3
No growth defect at 37°C
ΔPfAP2-HS
Poor growth at 37°C
Slow IDC progression
Reduced hsp70-1 and hsp90 levels
High sensitivity to proteotoxic stress (e.g. by ART) or proteasome inhibition
Strain-specific phenotype
Heat-Shock
Rapid PfAP2-HS-driven response
Misfolded proteins
TdGbox
PfAP2-HS
hsp70-1
hsp90
(PF3D7_1421800)
Other responses
Other TFs
Other chaperones
Other genes
ΔPfAP2-HS & PfAP2-HS_ΔD3
No rapid induction of hsp70-1 and hsp90
Low heat-shock survival
Increased cell damage and activation of other chaperones
Conserved phenotype
b
P. gallinaceum
P. gaboni
P. reichenowi
P. falciparum
P. vinckei
P. chabaudi
P. berghei
P. yoelii
P. vivax
P. cynomolgi
P. knowlesi
P. ovale
P. malariae
c
D1
D2
D3
P. falciparum
P. reichenowi
P. gaboni
P. gallinaceum
P. vivax
P. cynomology
P. knowlesi
P. ovale
P. malariae
P. berghei
P. yoelii
P. chabaudi
P. vinckei

Extended Data Fig. 1

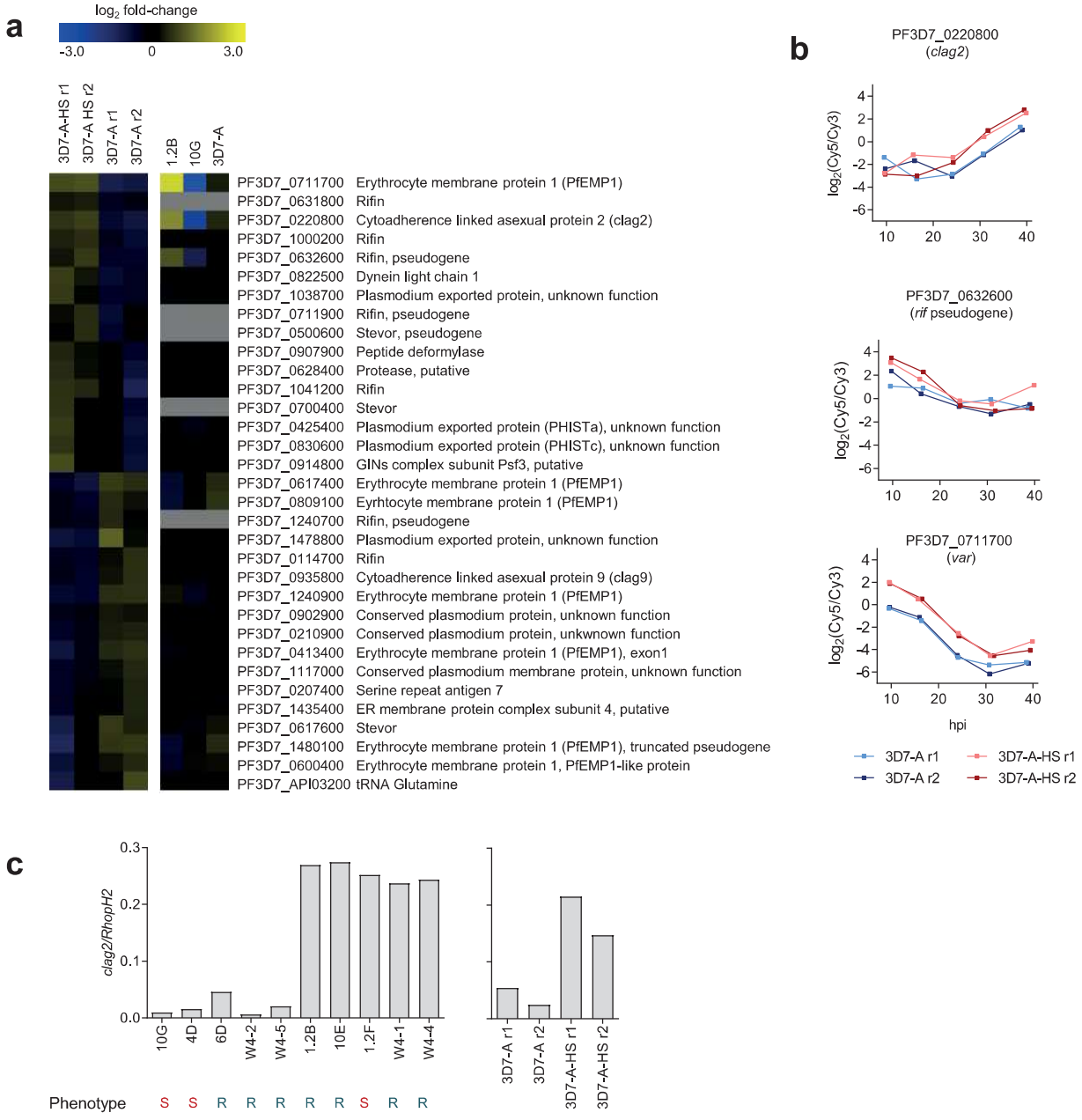

Extended Data Fig. 2

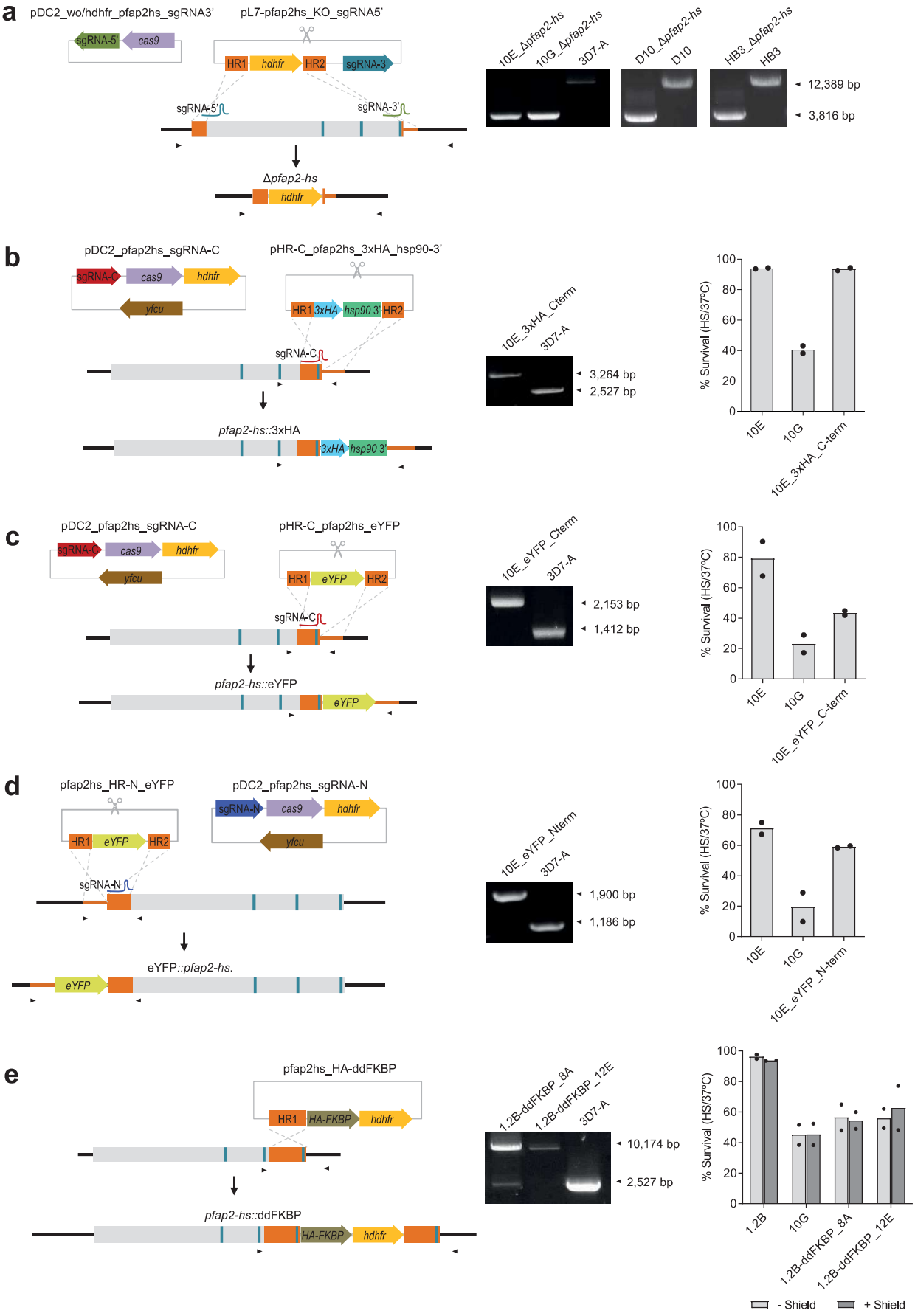

Extended Data Fig. 3

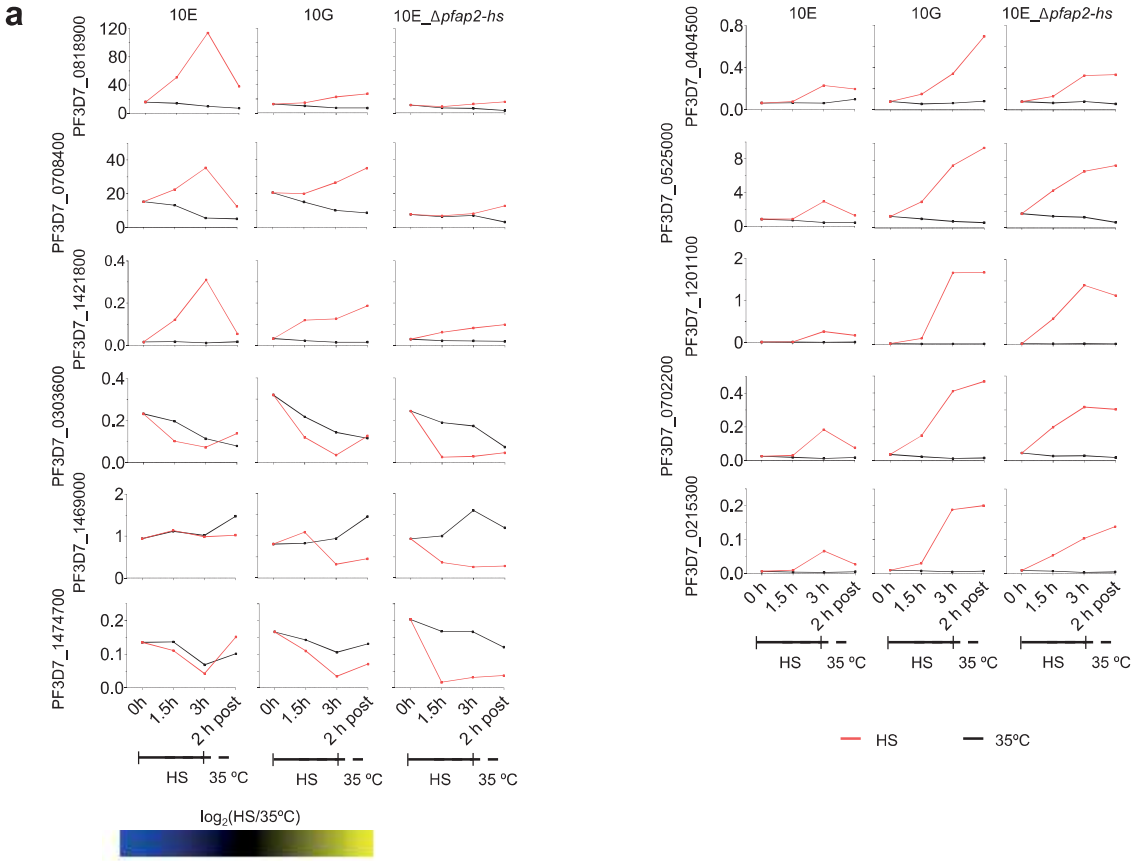

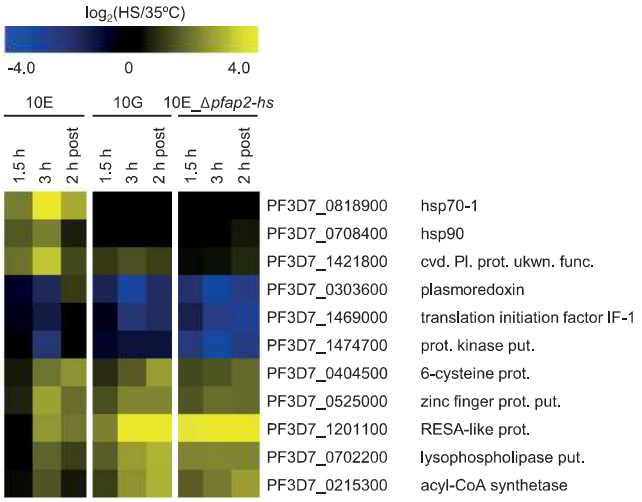

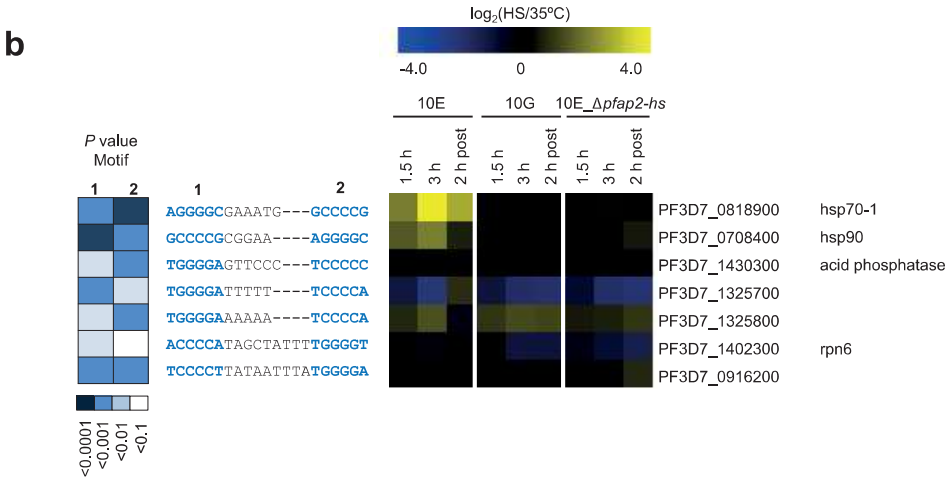

Extended Data Fig. 4

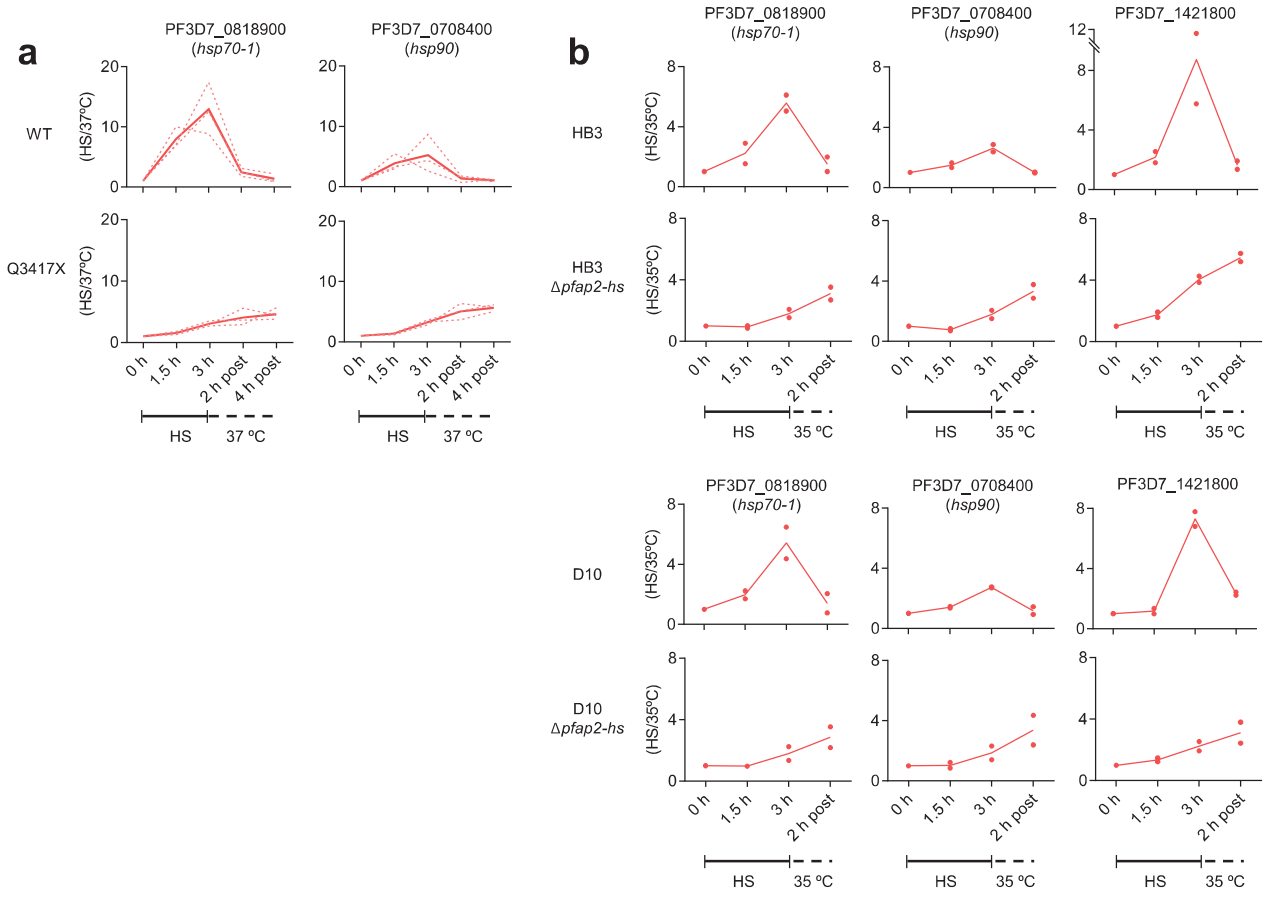

Extended Data Fig. 5

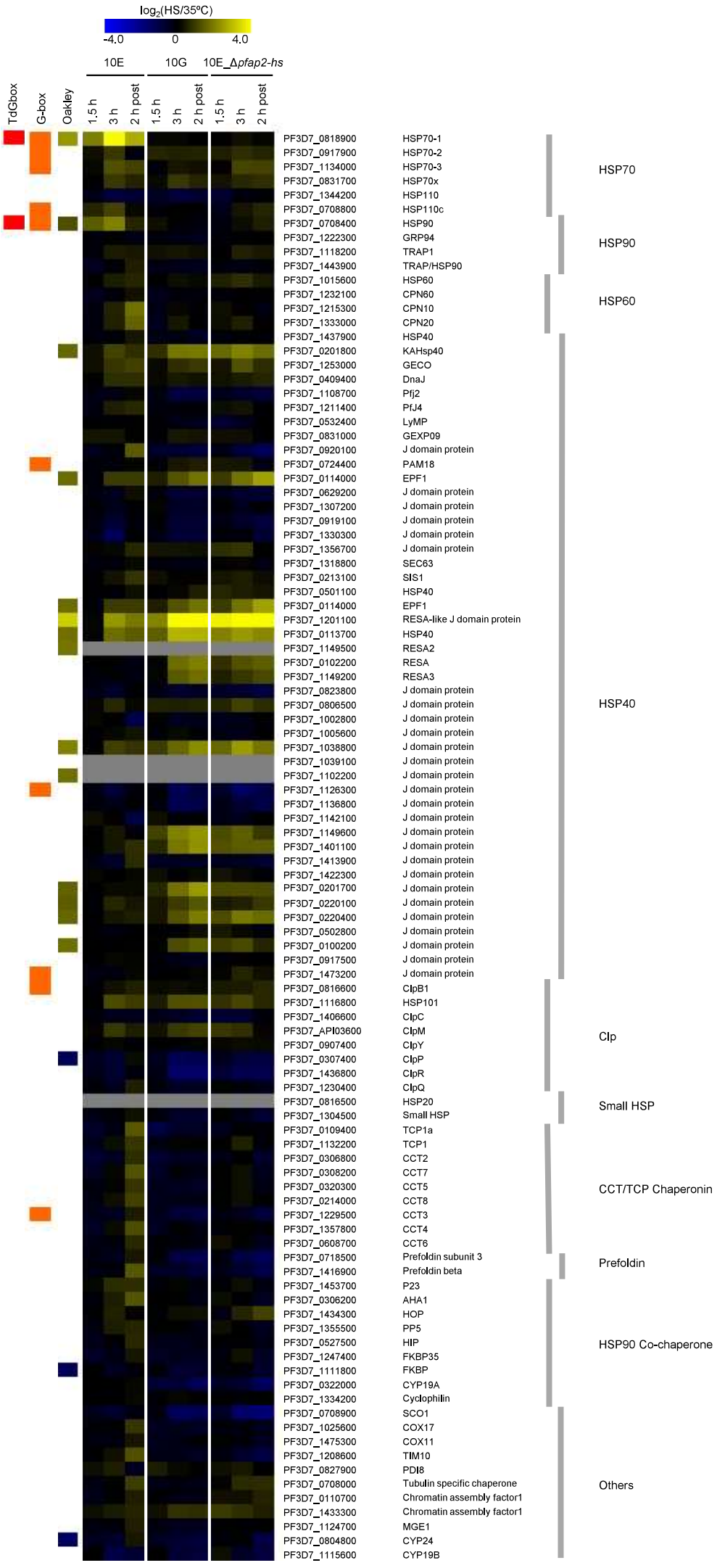

Extended Data Fig. 6

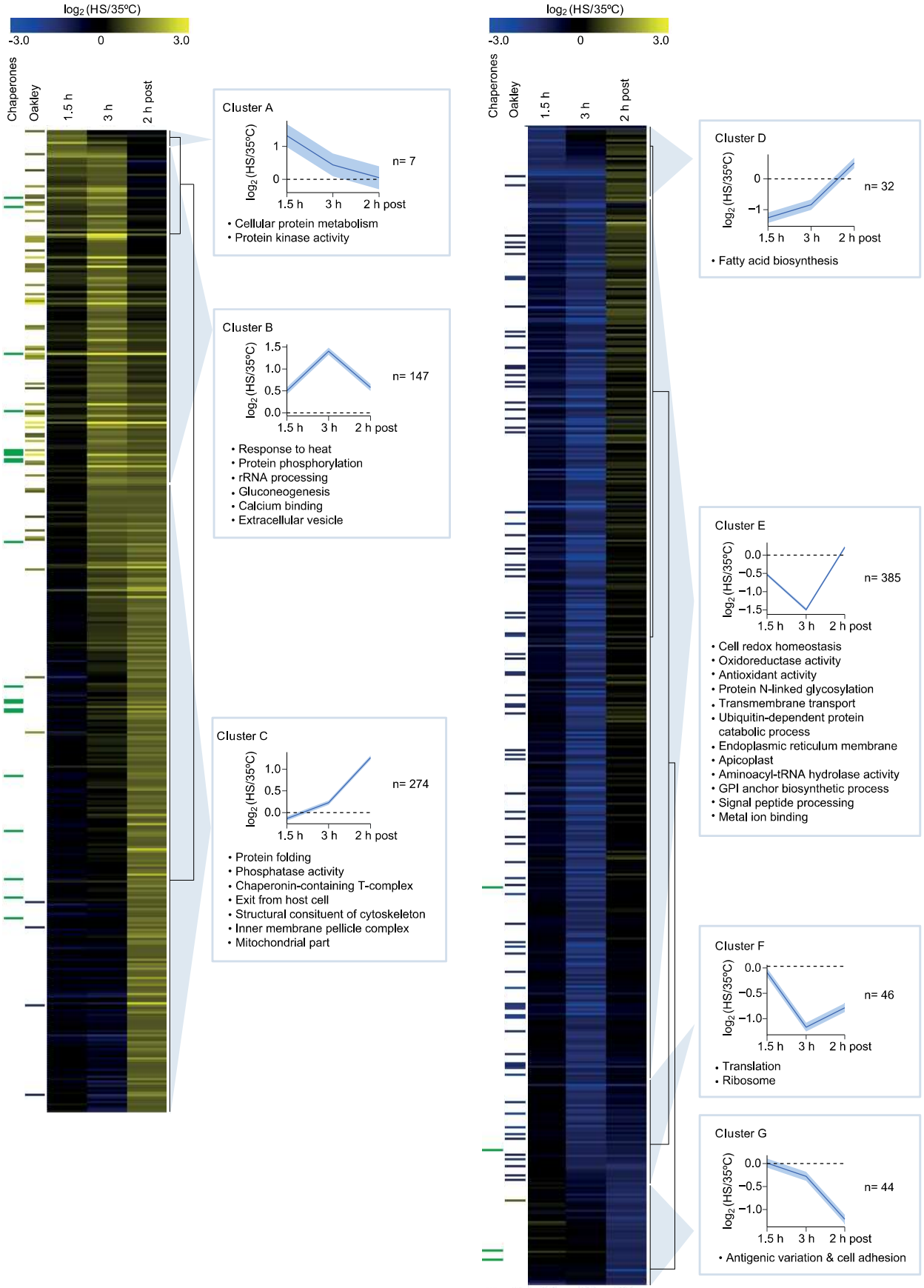

Extended Data Fig. 7

a

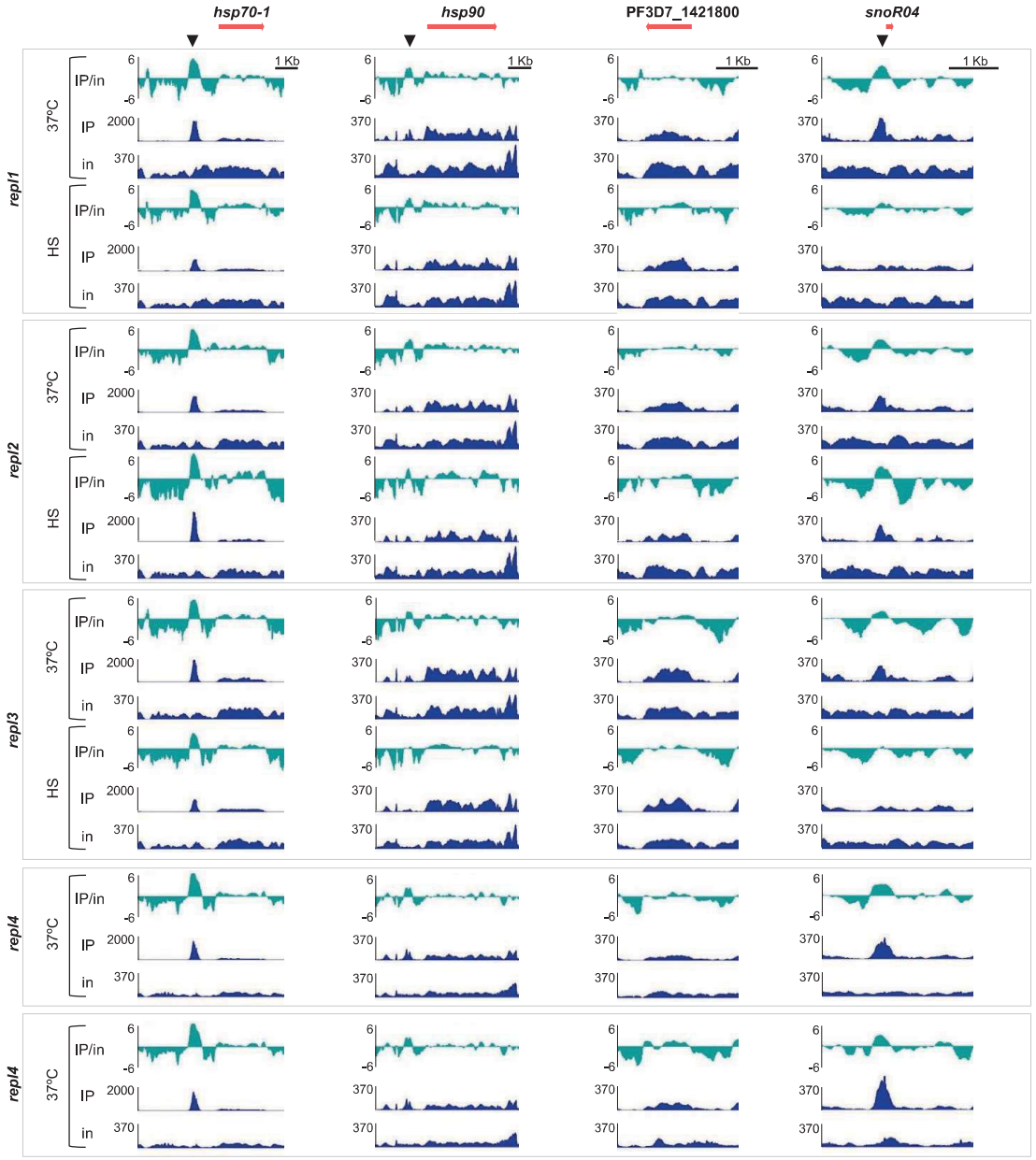

b

	Chrom.	Start	End	Median MACS2 Score	Median Fold Enrich.	Closest Gene	Gene Name	Location
Control	8	859109	859513	3155	14.6	PF3D7_0818900	*hsp70-1*	5'
	5	465548	465850	429	4.2	PF3D7_0510900	*snoR04*	5' & gene body
	13	2895119	2897998	150	2.3	Telomere	-	--
HS	8	859123	859514	3410	21.8	PF3D7_0818900	*hsp70-1*	5'
	10	1437164	1437430	226	3.5	PF3D7_1036400	*lsa1*	Gene body
	13	2909970	2912982	181	2.9	Telomere	-	-

c

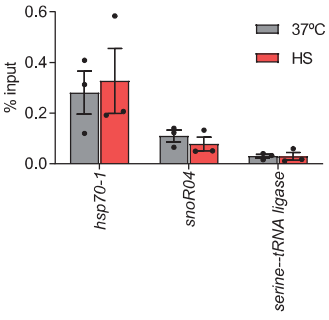

Extended Data Fig. 8

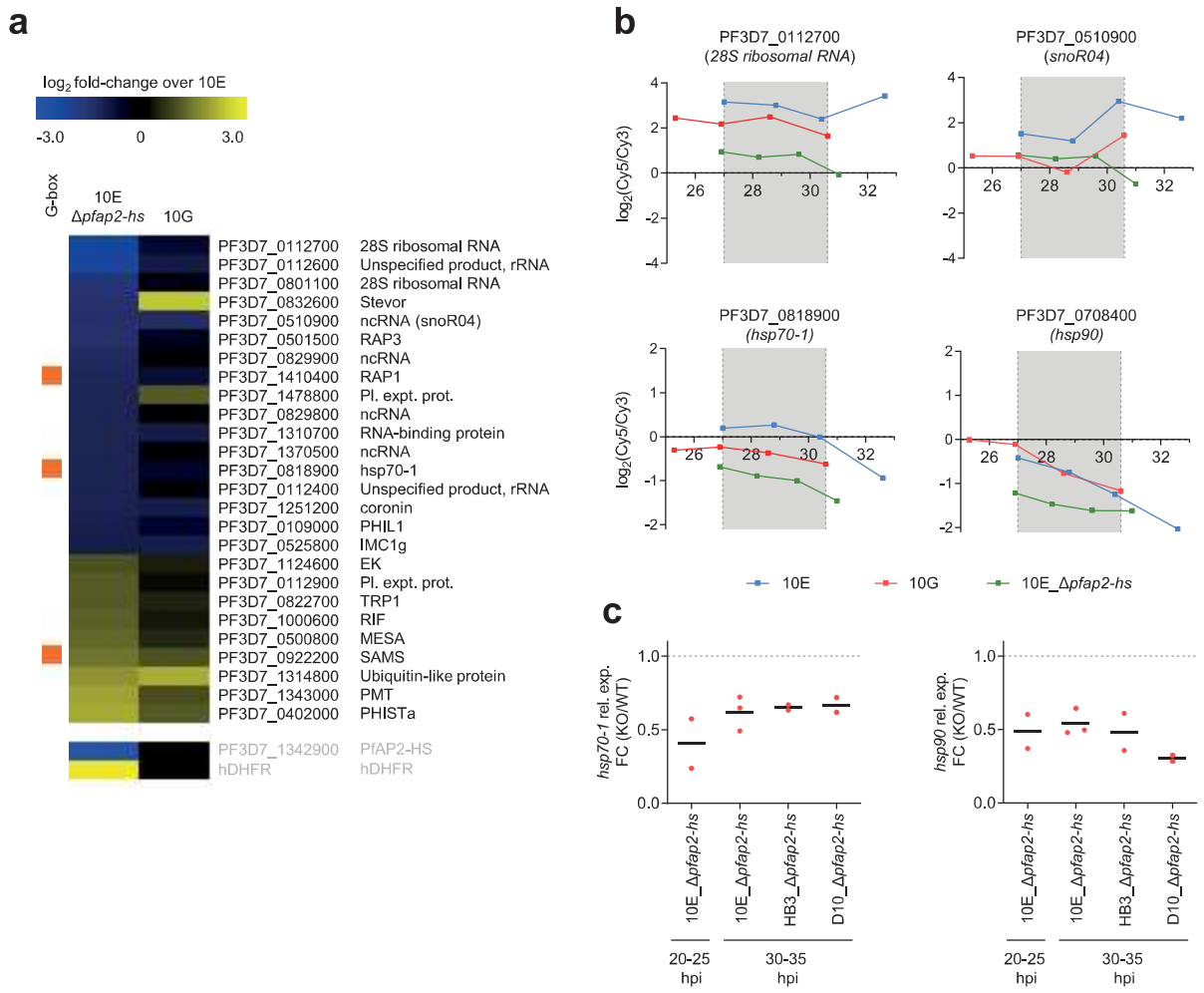

Extended Data Fig. 9

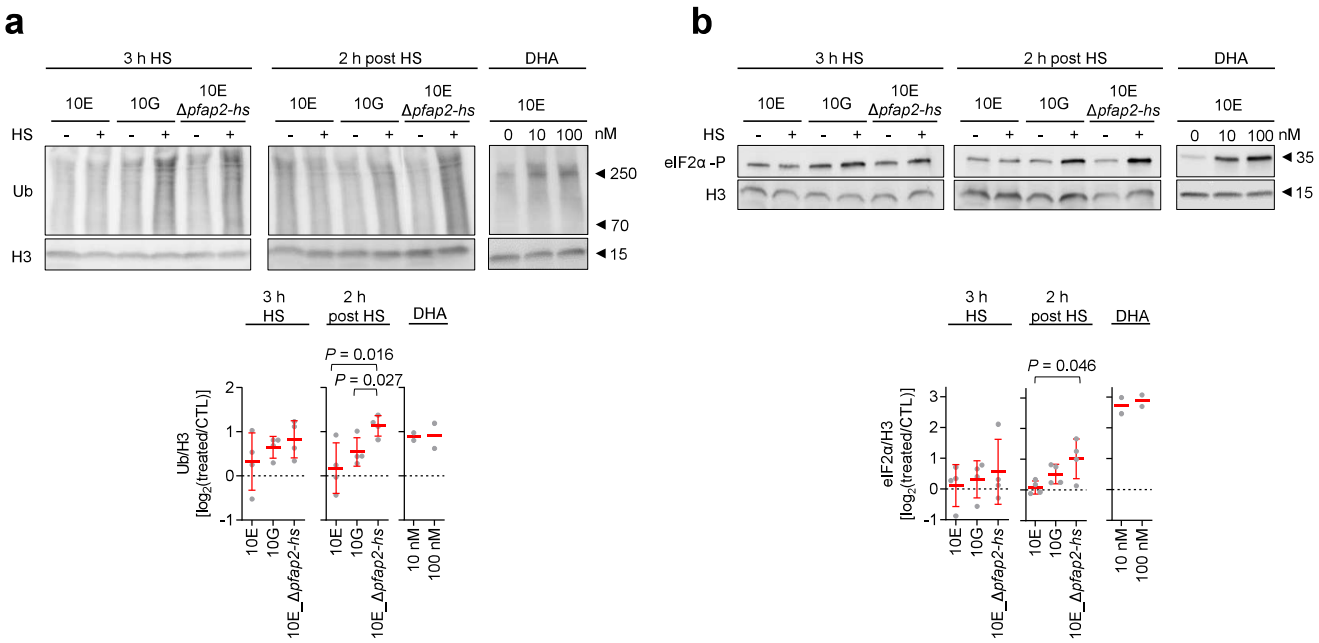

Extended Data Fig. 10